Quantification of hydraulic trait control on plant hydrodynamics and risk of hydraulic failure within a demographic structured vegetation model in a tropical forest (FATES-HYDRO V1.0)

Chonggang Xu[1], Bradley Christoffersen[2], Zachary Robbins[1], Ryan Knox[3], Rosie A. Fisher[4], Rutuja Chitra-Tarak[1], Martijn Slot[5], Kurt Solander[1], Lara Kueppers[3,6], Charles Koven[3], Nate McDowell[7,8]

1: Earth and Environmental Sciences Division, Los Alamos National Laboratory, Los Alamos NM, USA

2: ~~Biology Department~~School of Integrated Biological and Chemical Sciences, University of Texas Rio Grande Valley, ~~TA~~TX, USA

3: Lawrence Berkeley National Laboratory, Berkeley, CA USA

4. CICERO Centre for International Climate Research, Oslo, Norway

5: Smithsonian Tropical Research Institute, Apartado 0843-03092, Balboa, Ancon, Republic of Panama

6: Energy and Resources Group, University of California, Berkeley, CA USA

7: Atmospheric Sciences and Global Change Division, Pacific Northwest National Laboratory, Richland, WA, USA

8: School of Biological Sciences, Washington State University, Pullman, WA, USA

Corresponding author: Chonggang Xu (cxu@lanl.gov)

Style Definition: Comment Text

Abstract: Vegetation plays a key role in the global carbon cycle and thus is an important component within Earth system models (ESMs) that project future climate. Many ESMs are adopting methods to trace theresolve plant size and succession stage structure of plants withinecosystem disturbance history using vegetation demographic models. These models make it feasible to conduct more realistic simulation of processes that control vegetation dynamics. SeparatelyMeanwhile, increasing understanding of the ecophysiological processes governing plant water use, and the need to understand ecosystem responses to drought in particular, has led to the adoption of physicaldynamic plant water transport (i.e., hydrodynamic) schemes within ESMs. However, the impact of plant hydraulic trait variation in trait-diverse tropical forests is understudied. In this study, we report on a newsensitivity analysis of an existing hydrodynamics (HYDRO) model that is updated and incorporated ininto the Functionally Assembled Terrestrial Ecosystem simulator (FATES). The size and canopy structured representation within FATES is able to simulate how plant size and hydraulic traits affect vegetation dynamics and carbon/water fluxes. To better understand this new model system and its functionality in tropical forest systems in particular, we conducted a global parameter sensitivity analysis at Barro Colorado Island, Panama. We assembled 942 observations of plant hydraulic traits on 306 tropical plant species for stomata, leaves, stems, and roots, and determined the best-fit statistical distribution for each trait. Our , which was used in model analysis parameter sampling to assess the parametric sensitivity. We showed that the taper component determining , for simulated leaf water potential and loss of hydraulic conductivity tapering from trunk to branchacross different plant organs, the water potential leading to 50% loss (P_{50}) of four most important traits were associated with xylem conduit taper (buffers increasing hydraulic resistance with tree height), stomatal conductance, the sensitivity to leaf water potential, maximum stem hydraulic conductivity for the stem, and the

Formatted: Font color: Auto

Formatted: Font color: Auto

Formatted: Font color: Auto

~~fraction~~partitioning of total hydraulic resistance ~~in the above ground section are the top 5 traits determining the simulated water potential and loss~~ above vs. belowground. Our analysis of ~~conductivity for different plant organs. For the~~individual ensemble members revealed that trees at a high risk of hydraulic failure and potential tree mortality~~, we found that ensemble members with high risk of mortality~~ generally have ~~a higher taper exponent~~higher conduit taper, maximum xylem conductivity, stomatal sensitivity to leaf water potential, and ~~a higher xylem conductivity, less negative P_{50} for stomata conductance, and more negative P_{50}~~lower resistance to xylem embolism for stem and transporting roots. We expect that our results will provide guidance on future modeling studies using plant hydrodynamic models to predict the forest responses to droughts, and future field campaigns that aim to better parameterize ~~the~~ plant hydrodynamic ~~model~~models.

1. Introduction

Tropical forests play a critical role in regulating regional and global climates (Bonan, 2008). Under ongoing and future climate change, they are subjected to substantial risks of climate extremes such as drought and heat waves (Mcdowell et al., 2018). Studies have already shown that tropical forests were experiencing elevated tree mortality rates due to mega droughts related to ENSO events. For example, the 2015–16 El Niño led to the death of an estimated 2.5 ± 0.3 billion stems in the Lower Tapajós river basin of the Amazon and the associated carbon loss had not yet been compensated by new plant growth three years after the event (Berenguer et al., 2021). ~~Such extreme climate events are projected to increase in frequency and intensity under a warming future.~~Such extreme climate events are projected to increase in frequency and intensity under a warming future (Seneviratne et al., 2021). A statistical analysis based on the projection of 13 ESMs under a high greenhouse emission scenario showed that the frequency of extreme droughts as defined by rhizosphere soil moisture (occurring once every 50 years) could increase by a factor of nearly ~~4~~four and this increase would have ~~substantially more~~a disproportionate impact on tropical forests (Xu et al., 2019). The high species diversity found in tropical forests may result in increased resilience to climate extremes, based on the demonstrated resilience of temperate forests in relationship to trait diversity (Anderegg et al., 2018). However, due to limited data to ~~parametrize~~parameterize and constrain models for tropical forests, there is a large uncertainty in our predictive understanding of how tropical forests will respond to these climate extremes (Bonal et al., 2016). This tropical forest uncertainty is ~~considered to be~~ a key source of the global uncertainty in ~~our projection~~projections of land carbon fluxes and future climates (Arora et al., 2020).

Earth System Models (ESMs) have been developed to project future changes to the coupled climate and biosphere system. Typically, 'big leaf' approximations of vegetation with no explicit presentation of tree size and canopy structure have been used to predict the impact of vegetation on carbon and water cycles. These models do not represent the fundamental elements of vegetation dynamics including growth, mortality, competition~~, and growth~~, and their response to disturbances. In the last decade, many ESMs have incorporated vegetation demographic models (VDMs) that represent plant size, canopy structure and disturbance histories, with the goal of better representing the competitive dynamics among different size classes of trees and plant functional types in response to climate and ~~vegetation disturbance~~disturbances (Fisher et al., 2018). Most of these VDMs can differentiate plants' light, water and carbon use strategies and can thus represent some part of the functional diversity of tropical forests (Massoud et al., 2019; Koven et al., 2020).

Following the 'big leaf' model, water limitation on plant gas exchange in these VDMs is generally calculated based on three factors: 1) soil water potential; 2) root distribution; and 3) water potential for stomata openness and closure, all of which differ by plant functional ~~type~~types (Koven et al., 2020). While ~~such~~these soil-moisture-dependent water limitation functions are able to capture trait diversity in leaf-level stomatal behaviors, they fail to capture plant functional diversity in many other observable plant hydraulic traits, such as xylem capacitance, water potentials for loss of xylem hydraulic conductivity, stem hydraulic safety margin, and turgor loss point (Hochberg et al., 2018). Many studies have shown that plant hydraulic traits play an important role in plant responses to droughts (Su et al., 2022; Anderegg

Formatted: Font color: Black

et al., 2016), which could shape the landscape distribution of plant functional types (Kunert et al., 2021). In view of this limitation, plant hydrodynamic models have been developed with the aim of better simulating forest response to droughts (Powell et al., 2018; Christoffersen et al., 2016; Xu et al., 2016; Kennedy et al., 2019; Mcdowell et al., 2013)~~. These models not only allows us to better incorporate hydraulic functional diversity, but also allow us to mechanistically simulate the risk of plant mortality due to hydraulic functional failure resulting from embolism in xylem.~~. These models not only incorporate hydraulic functional diversity, but also mechanistically simulate the risk of plant mortality due to hydraulic functional failure, as a result of an inability to move water in the xylem due to embolism in conduits (Hammond et al., 2019).

One key challenge for these plant hydrodynamic models is that they have many more parameters than simple water limitation functions based on soil water potentials and thus inherently possess more uncertainty in the model parameterization and subsequent simulations. In this study, we describe the implementation of a hydrodynamic scheme within DOE-sponsored functionally assembled terrestrial ecosystem simulator (FATES~~,~~) (Koven et al. 2020), and assess this new configuration with two goals: 1) ~~assess~~quantify the ~~importance~~parametric sensitivity of different hydraulic traits in determining plant hydrodynamics; and 2) identify key hydraulic traits that are important for predicting the risk of mortality due to hydraulic failure. We expect that our results will provide guidance on model parameterization for future modeling studies using plant hydrodynamic models to predict tropical forest response to droughts, and future field campaigns that aim to collect observational data that can be used to better parameterize and benchmark plant hydrodynamic models.

2. Methodology

2.1. Model description

We use ~~the functionally assembled terrestrial ecosystem simulator (FATES),~~FATES, a VDM that is coupled within the Energy Exascale Earth System Model (E3SM) (Caldwell et al., 2019). FATES represents size-structured groups of plants (cohorts) and successional trajectory-based patches using the ecosystem demography approach (Fisher et al., 2015; Moorcroft et al., 2001). FATES simulates growth by integrating photosynthesis across different leaf layers for each cohort. FATES allocates this photosynthate to different tissues including leaves, fine and coarse roots, and stem, based on the allometry of different plant functional types, as well as a carbon storage pool (Fisher et al., 2015). Mortality within FATES is simulated by several mechanisms, including carbon starvation caused by depletion of the storage pool, hydraulic function failure, as well as impact mortality during disturbance, fire, logging, freezing, age-related and 'background' constant turnover (Fisher et al., 2015; Huang et al., 2020; Fisher et al., 2010; Needham et al., 2020).

2.1.1. Plant Hydrodynamics

The default (non-hydrodynamic) FATES model contains a simplistic algorithm that approximates plant hydraulic failure thresholds based on soil water potential. An important feature of the plant hydrodynamic scheme (HYDRO), which explicitly simulates water flow from the soil through leaves to the atmosphere, is that it enables direct representation of percent loss of conductance as a predictor of hydraulic failure mortality rates.~~-~~ FATES-HYDRO is based on the hydrodynamic model implemented in the Traits-based Forest Simulator (TFS) (Christoffersen et al., 2016)~~. The water flow is calculated based on water pressure gradients across different plant compartments (rhizosphere, absorbing roots, transporting roots, stem,~~

and leaf). and the features most relevant to the present analysis are summarized below. The model approximates water transport in a single vertical dimension, approximating the canopy as a single leaf layer at the top of a beam, according to the Shinozaki pipe model (Shinozaki et al., 1964) in which the hydraulic path length from the trunk base to each leaf is assumed constant. Following the 'porous media' approach, the model simulates the water transport across four main organs (leaves, stem- trunk/branches, transporting roots, and absorbing roots) and different rhizosphere shells (Fig. 1). Resistors connect the different compartments. Specifically, flow between compartment *i* and *i* + 1 (Q_i) is given by

The water flow is calculated based on water pressure gradients across different compartments (rhizosphere, absorbing roots, transporting roots, stem, and leaf). Specifically, flow between compartment *i* and *i* + 1 (Q_i)

$$Q_i = -K_i \Delta h_i, \quad (1)$$

is given by,

$$Q_i = -K_i \Delta h_i, \quad (1)$$

where K_i is the total conductance (kg MPa^{-1} s^{-1}) at the boundary of compartments i and $i+1$ and Δh_i is the total matric potential difference between the compartments:,

$$\Delta h_i = \rho_w g(z_i - z_{i+1}) + (\psi_i - \psi_{i+1}), \quad (2)$$

$$\Delta h_i = \rho_w g(z_i - z_{i+1}) + (\psi_i - \psi_{i+1}), \quad (2)$$

where z_i is compartment elevation difference above (+) or below (-) the soil surface (m), ρ_w is the density of water (10^3 kg m^{-3}), g is acceleration due to gravity (9.8 m s^{-2}), and ψ_i is tissue or soil matric water potential (MPa). K_i is treated here as the product of a maximum boundary conductance between compartments i and $i+1$ ($K_{max,i}$), and the fractional

Formatted: Font color: Auto

Formatted: Left

maximum hydraulic conductance of the upstream compartments (FMC_i or FMC_{i+1}), which is a function of the tissue water content. as follows,

$$FMC_i = \left[1 + \left(\frac{\psi_i}{P_{50,x}}\right)^{a_x}\right]^{-1} \quad (3)$$

where ψ_i is the compartmental water potential, $P_{50,x}$ is the water potential at 50% loss of maximum conductivity for different plant tissues (absorbing root, transporting root, stem), a_x is the corresponding vulnerability curve shape parameter, with a larger number indicating a steeper reduction of conductivity in response to more negative water potentials (Choat et al., 2012). The maximum percentage loss of conductivity (PLC) across different organs [i.e., PLC_i =100 (1-FMC_i)] is used to measure the risk of tree mortality (M_{hf}) resulting from hydraulic failure as follows,

$$M_{hf} = M_{hf,base}\frac{\max(0,\ PLC_{max,organ} - PLC_c)}{100 - PLC_c}, \quad (4)$$

where PLC_c is the critical percentage loss of conductivity with risk of mortality, $PLC_{max,organ}$ is the maximum percentage loss of conductivity across different organs, $M_{hf,base}$ is the baseline mortality rate [fraction/year] when percentage loss of conductivity exceeds PLC_c. In this version of model, we assume that xylem cavitation can fully recover as long as the trees do not die.

The previous version of this model (TFS-Hydro) presented water in terms of relative water content (RWC; g H_2O g^{-1} H_2O at saturation) in line with most empirical work on plant water relations. While the underlying equations remain unchanged, here we present water in terms of volumetric water content (θ; m^3 H_2O m^{-3} plant tissue), since this what is accounted by the model and is consistent with what is tracked in the soil as well. The two quantities are related via the equation RWC = θ/θ_{sat}, where θ_{sat} indicates saturated volumetric water content. The water potential for tissue x [ψ_x] is related to θ_x (the PV curve) following three stages of water tissue drainage as follows (Tyree and Yang, 1990; Bartlett et al., 2012),

$$\psi_x = \begin{cases} \psi_{0,x} + m_{cap}\left(\frac{\theta_x}{\theta_{sat,x}} - 1\right) & \theta_{ft} < \theta_x \leq \theta_{sat,x} \\ \psi_{sol}(\theta_x) + \psi_p(\theta_x) & \theta_{tlp,x} < \theta_x \leq \theta_{ft,x} \\ \psi_{sol}(\theta_x) & \theta_{r,x} < \theta_x \leq \theta_{tlp,x} \end{cases} \qquad (5)$$

Stage one applies to stem and roots only and represents the water draw from capillary reserves (embolized conduits or airspaces in wood) when wood water content is in between full turgor ($\theta_{ft} = RWC_{ft}\,\theta_{sat,x}$) and saturation ($\theta_{sat,x}$) and only represents a small fraction of the total PV curve. It is linear with constant slope m_{cap} = 11.3 MPa m^3 m^{-3} and RWC_{ft} = 0.958 as estimated from sapwood PV curves on 28 tropical and subtropical species (Christoffersen et al. 2016). RWC_{ft} is assumed to be 1.0 in leaves. Xylem water potential is assumed zero at full saturation. The second stage is between full turgor ($\theta_{ft,x}$) and the turgor loss point ($\theta_{tlp,x}$), when the xylem water potential is in balance with solute ($\psi_{sol}[\theta_x]$) and pressure water potential ($\psi_p[\theta_x]$) of living cells. The third stage is after the turgor loss point ($\theta_{tlp,x}$), but above the point of residual water content ($\theta_{r,x} = RWC_{r,x}\,\theta_{sat,x}$) where the water potential is only a function of the solute water potential. $RWC_{r,x}$ is synonymous with the apoplastic fraction (Bartlett et al. 2012).

The solute water potential is given as,

$$\psi_{sol}[\theta_x] = \frac{\pi_0(\theta_{sat,x}RWC_{ft} - \theta_{r,x})}{(\theta_x - \theta_{r,x})}, \qquad (6)$$

where π_0 is the tissue osmotic potential at full turgor. The pressure potential is calculated as follows,

$$\psi_p[\theta_x] = -|\pi_0| + \varepsilon\frac{(\theta_x - \theta_{sat,x}RWC_{ft})}{(\theta_{sat,x}RWC_{ft} - \theta_{r,x})}, \qquad (7)$$

where ε is the bulk elastic modulus (MPa).

The realized conductivity of the above ground portion of the plant per unit of leaf area ($K_{l,max,tree,ag}$) is calculated based on xylem hydraulic conductivity at petiole ($k_{s,max,petiole}$), aboveground tree height (H, meters), and a xylem taper factor (X_{tap}) as follows,

$$K_{l,max,tree,ag} = \frac{k_{s,max,petiole}}{H(\frac{A_l}{A_s})} X_{tap}, \qquad (8)$$

where $k_{s,max,x}$ is the maximum xylem conductivity per unit sapwood area, $\frac{A_l}{A_s}$ [i.e., la2sa in Table 1] is the ratio of leaf area (A_l) to sapwood area(A_s). X_{tap} is the xylem taper factor representing the ratio of aboveground xylem conductance with taper to that without, which for intermediate values of conduit taper (*p_taper* = 1/6; see below) represents a factor increase in total conductance of 23–50 for trees of heights 10–30 meters (Christoffersen et al., 2016). Savage et al. (2010) highlighted how opposing selective forces will both increase hydraulic conductance by the tapering of conduit radii (*p_taper* > 0) while at the same time protect against embolism by minimizing conduit taper (no taper implies *p_taper* = 0). They defined *p_taper* as the exponent on an external branching parameter (2 daughter branches per parent branch in their model) that sets the degree of internal branching of xylem conduits (and thus the tapering of conduit radii as well) and, using a fractal network model, derived an effective exponent *q* that describes how aboveground conductance increases with tree size. *q* is a monotonically increasing and saturating function of the taper exponent *p* (see Fig 2b of Savage et al. 2010); we used this relationship to estimate *q*, and thus X_{tap} in eq. (8) as

$$X_{tap} = \left[\frac{r_{base}}{r_{petiole}}\right]^{q_{tap}-q_{notap}}, \qquad (8)$$

where r_{base} and $r_{petiole}$ are the trunk and petiole radii, respectively. The ratio $r_{base}/r_{petiole}$ is related to tree height following the fractal tree model of Savage et al. (2010) (see equations S12-S13 in Christoffersen et al. 2016).

Eq. (8) only gives the aboveground component of whole-plant conductance. In the absence of a simple first-principles approach to estimating the belowground component, we estimate the total tree maximum conductance (above- and belowground components) as

$$K_{max,tree,total} = R_{frac,stem} K_{max,tree,ag}, \quad (9)$$

where $R_{frac,stem}$ is the fraction of total resistance that is aboveground.

Stomatal conductance [g_s, µmol m^{-2} s^{-1}] is simulated through a modified Ball-Berry equation,

$$g_s = g_0 + g_1 \frac{A_n}{C_s/P_{atm}} h_s, \quad (10)$$

where g_1 is the stomatal conductance slope in response to environmental condition changes, g_0 is the minimum (cuticular) stomatal conductance (µmol m^{-2} s^{-1}), C_s is the leaf surface CO_2 partial pressure (Pa), P_{atm} is the atmospheric pressure (Pa), h_s is the leaf surface humidity, and A_n is leaf net photosynthesis rate (µmol CO_2 m^{-2} s^{-1}). Stomatal conductance is further modified by a plant water stress factor, β, calculated as

$$\beta = [1 - \left(\frac{\psi_{leaf}}{P_{50,gs}}\right)^{a_{gs}}]^{-1}, \quad (11)$$

where ψ_{leaf} is the leaf water potential, $P_{50,gs}$ is leaf water potential at 50% loss of maximum stomatal conductance, and a_{gs} is the stomatal vulnerability shape parameter.

The total fine root surface area affects the amount of water a plant can take up through its influence on rhizosphere conductance and is determined by both the specific root length (srl) and absorbing root radius (*rs2*). Specifically, the model has a specified number of soil shells (5 in this study) around fine root surfaces and the conductance between soil shell *k+1* and *k* , $K_{shell,k}$, is calculated as,

$$K_{shell,k} = K_s \frac{\pi\, l_{aroot,common}}{\ln(r_{k+1}/r_k)}, \quad (12)$$

where r_k is the mean radi of kth shell, $l_{aroot,common}$ is the total length of absorbing roots calculated as a product of total fine root biomass and specific root length (*srl*). K_s is set to be the conductance for soil (K_{soil}) when k>1. For k = 1,

$$K_s = \frac{1}{\frac{1}{K_{soil}} + \frac{1}{K_{root\_soil}}}, \quad (13)$$

where K_{root_soil} is the conductance between fine root surface and soil. An update to the TFS-Hydro approach is to make this conductance direction-specific, in view that water loss rate from root could be substantially lower than water uptake rate either through osmatic regulation (Dichio et al., 2006) or by lacunae caused by rupture of cortical cells (North and Nobel, 1992) during drought. It is determined by either the maximum uptake of water per unit of absorbing root surface area ($k_{r1,max}$, kg m^{-1} s^{-1} MPa^{-1}) when root water potential is more negative than adjacent rhizosphere soil water potential, or the maximum root water loss rate per unit surface area ($k_{r2,max}$, kg m^{-1} s^{-1} MPa^{-1}) when rhizosphere water potential becomes more negative than root water potential, which may occur, for example, in frozen soils or in very dry soil layers (Schmidhalter, 1997).

The plant hydrodynamic representation and numerical solver scheme within FATES-HYDRO follows the 1-D solver laid out by Christoffersen et al. ((2016), which is the default solver in FATES-HYDRO and used in this study. The model also has an option of a 2-D solver, which is slower and detailed by Fang et al. (2022) and Lambert et al. (2022). 2016). The equations are solved for tissue water content at a 30 minutes time step. We made a few modifications to accommodate the multiple- soil layers and improve the numerical stability. First, to accommodate the multiple-soil layers, we sequentially solve the Richards' equation for each individual soil layer, with each layer-specific solution proportional to each layer's contribution to the total root-soil conductance. Second, to improve the numerical stability, we now linearly interpolate the pressure/volume curve beyond the residual and saturated tissue water content to avoid the rare cases of overshooting in the numerical scheme under very dry or wet conditions. ~~Please see~~See the Supplementary Information [HYDRO_DESCRIPTION.pdf] for further details of the implementation.

2.1.2. Non-hydrodynamics processes

FATES-HYDRO can be coupled to different host land models (HLMs) including the E3SM land model (ELM) (Caldwell et al., 2019) or the Community Terrestrial Systems Model (CTSM) (Lawrence et al., 2019). In this study, the model is coupled to ELM. In this section, we layout the key non-hydrodynamic processes in the FATES or the ELM for a better understanding of parameter importance in the results.

Canopy radiative transfer is calculated using a multi-layer scheme based on the iterative Norman radiation scheme (Norman, 1979). Leaf and stem area is binned into a matrix of canopy layer, leaf layer and plant functional types. Reflectance, absorption, and transmittance are calculated for each leaf layer. Between canopy layers, light streams are averaged between plant functional types (PFTs), such that all PFTs in understory layers receive equal radiation on their top leaf layer. Fractional absorption of visible and near infra-red light is calculated separately for direct and diffuse light. For the direct stream, transmitted and reflected light is converted into diffuse fluxes. In FATES, the absorbed PAR is used to calculate photosynthesis rates for each of the canopy layer x leaf layer x PFT bins, after which rates across layers are re-aggregated into cohort level carbon fluxes. Please see the Supplementary file in Fisher et al. (2015) for details.

The energy balance is handled by the host land model. In this study, it is based on the land component of DOE's Exascale Energy Earth System Model (E3SM). The E3SM land model

(ELM) is based on the Community Land Model 4.5 (Oleson, 2013). Specifically, in ELM, the average canopy temperature is calculated based on the energy balance of latent heat, sensible heat, and absorbed radiation as determined by the radiative transfer model. The latent heat is determined by the transpiration, which is determined by the vapor pressure deficit from inside of leaf to the air, canopy stomatal conductance, and boundary layer conductance. FATES calculated mean canopy stomatal conductance averaged across different cohorts, which is fed to ELM to calculate the energy balance. The Newton-Raphson numerical scheme is used to solve for the canopy temperature.

All aspects of soil water balance (infiltration, water transfer among soil layers, and drainage) happen at the 'column' scale at 30-min time steps and are handled within the Host Land Model (see Oleson et al. 2013 for a detailed description of hydrology in CLM4.5, the parent model of ELM). FATES-HYDRO handles soil water operations at the patch and cohort scales. It simulates root water uptake and changes in plant water potential from roots to leaves based on current time step transpiration. The belowground conductance for each soil layer is weighted by root biomass with an exponential vertical distribution. Sections 2 and 3 in the Supplement of this manuscript provide full details on boundary conditions, sequence of operations among HYDRO and the HLM, downscaling of soil moisture to rhizosphere shells, and downscaling of transpiration from the patch to individual scale.

2.2. Sensitivity analysis

~~In this study, as our focus is on the plant hydrodynamics, we used the static stand structure mode of FATES that turns off the processes of competition, growth and mortality, to instead hold the ecosystem structure constant. This reduced-complexity configuration (Fisher and Koven, 2020) thus exercises only the primarily fast-timescale processes of photosynthesis,~~

Field Code Changed

transpiration, water transport, and plant hydrodynamics (i.e., change in hydraulic conductivity, water storage, and water potentials in plant tissues). By using static stand structure mode, as in Chitra-Tarak et al. (2021), we isolate hydraulic trait controls on simulated hydrodynamics and avoid confounding, and potentially biased, feedbacks from resulting changes in forest structure. The forest stand structure include tree size and composition is initialized based on the forest inventory data in 2017. As the majority of species in BCI is evergreen broad leave trees, we run the model with one PFT with different hydraulic traits (Table 1) to assess their impact on the hydrodynamically relevant outputs including water potentials and fraction of maximum conductivity for different plant organs including absorbing root, transporting root, stem, and leaves and risk of hydraulic failure. FATES simulates the carbon and water fluxes for different size classes of trees. Because large trees experience more fluctuation in environmental conditions in the canopy, here we focused on hydrodynamic behaviors for trees of diameter more than 60 cm.

Field Code Changed

2.2. Parametric uncertainty estimation

We identified 3635 parameters for the FATES-HYDRO model to conduct the parametric sensitivity analysis (Table 1). To estimate the parameter distributions, we started with published meta-analyses (Christoffersen et al., 2016; Choat et al., 2012; Bartlett et al., 2012; Bartlett et al., 2014; Bartlett et al., 2016; Klein, 2014) and supplemented them with select new data from individual studies. Focal data were tissue- or individual-level hydraulic traits spanning water transport and embolism resistance, tissue water storage and retention (PV curve traits), hydraulic architecture (i.e., leaf area to sapwood area ratio), stomatal responses to dehydration, and fine root traits (Table 1). For each dataset, we standardized taxonomic names using the TNRS package in R (Boyle et al., 2013). This allowed us to join datasets together

Formatted: List Paragraph

based on species, averaging multiple observations per species if necessary, resulting in a species-specific sparse matrix of all hydraulic traits for all databases and individual studies that we compiled. This pantropical hydraulic trait dataset is included in the Supporting Information [traits_master_trop.csv].

~~We then determined parametric~~

This trait dataset consisted of anywhere from 1 - 323 observations for each trait, where each observation corresponds to a different species (multiple observations for the same species are first averaged; see above). Before fitting distributions ~~which best fit the trait~~ to these data~~.~~ ~~Where necessary,~~, some traits were first transformed to be positive~~, and certain traits with well-defined~~ (e.g., P50) or normalized within [0, 1] when upper and lower bounds were ~~normalized on [0, 1] according to (x – x.lowerbound)/(x.upperbound – x.lowerbound) for trait x~~ well-defined (Table 1). ~~For~~Then, for each trait separately, we used ~~parameter estimates for the~~ the fitdistr package in R to estimate best-fit parameters for uniform, beta, normal, lognormal, and gamma statistical distributions in order to estimate central tendencies and spread for each trait. The distribution with the largest log likelihood ~~among all possible distributions using fitdistr package in R.~~ and best-fit parameters are given in Table 1. Each model simulation consisted of a single PFT: all trees (across all cohort sizes and patches) had the same traits.

We augmented observations with extratropical data to increase sample size for traits with less than three tropics-specific observations. ~~Where~~When trait data observations were ~~mostly unmeasured~~not present, we used a uniform distribution bounded on our best estimate of the theoretical range (Table 1). As there is limited data on roots, we used the same distribution as that for branches if data ~~was missing~~were lacking. Because our goal is to understand the model behaviors as determined by different hydraulic traits, we assumed independence among traits.

Formatted: List Paragraph

As we focused on the hydraulic traits in this study, we used non-hydraulic trait values based on an optimal set of parameters that best fit observed water and carbon fluxes in a set of FATES ~~implemented~~simulations run without hydrodynamics (Koven et al., 2020).

~~**2.3.1.1. Sensitivity analysis**~~

We used the Fourier Amplitude Sensitivity Test (FAST) to assess the relative importance of parameters in determining the variance of model outputs (Xu and Gertner, 2011a). The main idea of FAST is to assign periodic signals in the sampled parameter values and use Fourier transformation to identify the signals in the outputs. Sampled parameter values are based on Latin hypercube sampling from the fitted statistical distributions (see previous section for more details). We ran 1000 ensemble simulations of the FATES-Hydro to derive model outputs of water potential and fraction of maximum conductivity. For each ensemble simulation, each plant hydraulic trait was assigned with a random draw from each trait's distribution, and the samples for different traits are randomly combined to sample the observed plant hydraulic trait space for sensitivity analysis.

We used the Uncertainty Analysis and ~~Sensitivyt~~Sensitivity Analysis (UASA) tool (https://sites.google.com/site/xuchongang/uasatoolbox) to estimate the ~~parameter importance~~parametric sensitivity index, which is ~~defined as~~calculated based on the ~~proportion~~ratio of ~~total~~ the partial variance in the model output ~~variance contributed by individual~~attributed to a specific parameter to the total variables in the model ~~parameters~~output. For details, please refer to Xu and Gertner (2011a). We ~~run~~ran the model with 1000 ensemble members, in view that an order of 100 times effective important number of parameters, which we estimate to be ~10, is needed to achieve reasonable precision (Xu and Gertner, 2011b).

Formatted: Font color: Auto

~~2.4.~~2.3. Study area ~~and climate drivers~~

In this study, we used Barro Colorado Island (BCI), Panama, as our test site to evaluate model behavior. We chose BCI ~~as~~because it has moderately, strong dry and wet seasons that allow us to assess the hydrodynamics under different levels of water availability. Moreover, extensive field campaigns in recent years have provided comprehensive data needed for model parameterization, initialization and climate drivers. Finally, we also leverage prior FATES studies of non-hydraulic parameters at BCI (Koven et al., 2020).

BCI has an annual mean temperature of 26.3°C and an annual mean precipitation of 2656 mm with a strong seasonal precipitation signal. The dry season lasts from January to April, with a mean precipitation of 228mm, while the wet season lasts from May-December with a mean precipitation of 2428mm (Paton, 2020). In this study, we used hourly in-situ climate data from 2008-2016 to drive the model. To run the model to equilibrium (in terms of soil moisture content) takes 5-6 years, thus we choose February of 2016 as the target for analysis of dry season hydrodynamics and August of 2016 as the target for analysis of wet season hydrodynamics. ~~Using static stand structure mode means that we do not need to spin up vegetation state and thus reducing the simulation time.~~

2.4. Model setup

In this study, as our focus is on the plant hydrodynamics, we used the static stand structure mode of FATES that turns off the processes of competition, growth and mortality, to instead hold the ecosystem structure constant. This reduced-complexity configuration (Fisher and Koven, 2020) thus exercises only the primarily fast-timescale-processes of photosynthesis, transpiration, water transport, and plant hydrodynamics (i.e., change in hydraulic conductivity, water storage, and water potentials in plant tissues). By using static stand structure mode, as in

Formatted: Font: Times New Roman, 12 pt, Not Highlight

Field Code Changed

Chitra-Tarak et al. (2021), we isolate hydraulic trait controls on simulated hydrodynamics and avoid confounding, and potentially biased, feedbacks from resulting changes in forest structure. Using static stand structure mode also means that we do not need to spin up vegetation state, thus reducing the simulation time. The forest stand structure, consisting of tree size and composition for each patch, is initialized based on forest inventory data collected in 2015 (http://ctfs.si.edu/webatlas/datasets/bci/). As the majority of species in BCI are evergreen broad leaf trees, we ran the model with one PFT with different hydraulic traits (Table 1) to assess their impact on the hydrodynamically relevant outputs including water potentials and fraction of maximum conductivity for different plant organs including absorbing root, transporting root, stem, and leaves.

Field Code Changed

One key benefit of utilizing a hydrodynamic model is its ability to simulate the risk of hydraulic failure by considering the loss of conductivity in various plant organs. As FATES model was ran on static stand mode, we did not specifically simulate the tree mortality resulting from the hydraulic failure as shown in Eq. (4). Instead, we used the maximum of loss of conductance across the continuum of plant nodes [i.e., $PLC_{max,organ}$ in eq. (4)] to assess the hydraulic failure risk. If $PLC_{max,organ}$ reaches critical threshold PLC_c, which is set to 50% (Adams et al., 2017), trees are assumed to be faced with a high risk of mortality. Using the ensemble simulations, we also aim to identify the most vulnerable plant organs and the critical parameters that influence the likelihood of hydraulic failure.

FATES simulates the carbon and water fluxes for different size classes of trees. The forest has 137 cohorts with diameters ranging from 10 cm to >2 meters and height ranging from 1 to 38 meters (see Fig. S1 for size distributions). Because large trees experience more fluctuations in environmental conditions in the canopy and higher risk of mortality due to drought (Bennett et al., 2015), we focused on hydrodynamic behaviors for large trees with diameter at breast height (DBH) more than 60 cm; however, for comparison, we also derived the sensitivity for smaller trees with DBH less than 60 cm.

3. Results

Our results showed that the simulated ranges across the ensemble of leaf water potential (Fig. ~~1~~2) and loss of conductivity (Fig. ~~2~~3) are large. For leaf water potential of large trees with diameter > 60 cm, the 95% percentile ranges are from -5 MPa to -0.5 MPa and -3 MPa to -0.5 ~~Mpa~~MPa for February (dry) and August (wet) 2016, respectively. Correspondingly, the fraction of maximum stem hydraulic conductivity is much higher during August compared to February (Fig. ~~2~~3); however, in both months, the modeled range spans almost the full range of between 0 and 1. For smaller trees with diameter less than 60 cm, our results show that smaller tree experienced less negative water potential (Fig. S2 and Fig. 2) and lower loss of hydraulic conductivity (Fig. S3 and Fig. 3).

Based on the FAST sensitivity indices (i.e., the variance in model output contributed by different parameters), the key parameters that control the water potentials of different plant organs (leaf, stem and root) for large trees (diameter >60 cm) include the taper exponent for hydraulic conductivity (*p_taper*), the water potential leading to 50% loss of stomatal conductance (*p50_gs*), maximum hydraulic conductivity for the stem (*kmax_node_stem*), and the fraction of total hydraulic resistance in the above ground section (*rfrac_stem*), in decreasing order (Fig. ~~3~~4). For the fractional loss of conductivity, the most important parameter is the water potential leading to 50% loss of hydraulic conductance (P_{50}) for the corresponding organs (Fig. ~~4~~5). Other important parameters are similar to those for simulated water potentials. Notably, the organ-specific P_{50} values are more important for the dry month (February) compared to the wet month (August). For the wet month of August, *p_taper* is the dominant parameter controlling the pre-dawn and midday loss of hydraulic conductivity, while organ-specific P_{50} parameters are the second most important. For smaller trees with diameter less than 60 cm, the corresponding parametric sensitivity patterns are similar to those of larger trees (Fig. S4 and Fig. S5); however, compared to larger trees, the parametric sensitivity of *p_taper* for simulated leaf water potential becomes lower for smaller trees (Fig. 4 and Fig. S4).

In terms of the risk of hydraulic failure, out of the 1000 ensemble members, ~40~~-60~~% of the simulations for February and ~60% of simulation for August suggest that branches are the most vulnerable plant organ, based on highest loss of conductivity across the continuum from root to branch (Fig. ~~5~~6). For the dry month of February, roots are at greater risk in comparison to the wet season. If we consider the loss of conductivity more than 50% for February 2016 as a threshold for a high risk of mortality (Adams et al., 2017), then 53% of ensemble simulations reach this threshold. The key parameters affecting the risk of mortality, as measured by percentage difference in parameter values for ensemble members reaching 50% loss of conductivity or not, include the water potential leading to 50% loss of conductance for stomata (*p50_gs*), stem (*p50_node_stem*), and transporting roots (*p50_node_troot*), maximum hydraulic conductivity of stem (*kmax_node_stem*), and the taper exponent (*p_taper*) (Fig. ~~6~~7). Ensemble members with high risk of mortality generally have a higher *p_taper* and *kmax_node_stem*, less negative *p50_gs*, and ~~more~~less negative p50 for stem and transporting roots (Fig. ~~7~~8).

4. Discussion

Our analysis showed the importance of key plant hydraulic traits in simulating plant water potential and risk of hydraulic failure. This analysis identifies these parameters as potential targets of either model calibration or targeted measurement campaigns to achieve realistic simulations. In our sensitivity analysis, the most influential parameter for both water potential and loss of conductivity is the tapering of the radius of conduit with increasing plant height (*p_taper*). As *p_taper* increases, the conduit radius increases from the top of the tree to its base. According to Hagen-Poiseuille's equation, this increases the theoretical maximum total conductance. Low values of *p_taper* thus limit the adverse effects of tree height by increasing *k_max* along the whole continuum and reducing the soil-to-leaf water potential needed to maintain transpiration. Our inference is that *p_taper* represents an overarching property of plant architecture that influences the relative effect of each of the other ~~parameters with regard to hydraulic safety and efficiency. While *p_taper* is less directly related to plant adaptations to drought, the architecture of the plant itself determines the range of values that give rise to drought adaptive strategies.~~traits related to hydraulic safety and efficiency (Olson et al., 2021). The xylem architecture as determined by *p_taper* parameter could change in response to age and development stages (Rodriguez-Zaccaro et al., 2019), which is not considered in this study. Future studies evaluating the importance of this change to hydraulic functions could be useful to guide size-dependent growth and mortality. Another dimension of the hydraulic architecture with a critical role in determining both water potential and loss of conductivity, though to a much lesser degree, was the fraction of total tree resistance ~~within~~ that is belowground (i.e., of the ~~above ground stem (~~entire transporting and absorbing root system; 1- *rfrac_stem*). Generally, a plant will ~~maintain this resistance, matching~~match the growth of its trunk and crown ~~height~~ to maintain ~~total~~a degree of equilibrium in aboveground resistance as the distance water needs to travel increases (Yang and Tyree, 1993). In this study, due to the lack of data on the belowground resistance, we assigned a quite large range for this trait, which could be

~~impact~~impacted by many factors such as belowground root biomass, root network architecture, and ~~interaction~~interactions between ~~root~~roots, fungi and bacteria~~.~~ (Poudel et al., 2021; Bhagat et al., 2021).

Formatted: Font color: Auto

The second most sensitive parameter in determining loss of conductance was the leaf water potential at 50% loss of stomatal conductance (*p50_gs*). ~~The~~This parameter controls the water loss rate from ~~leaf and~~leaves, with a less negative value ~~provides~~providing protection from hydraulic failure during water~~-~~-limited periods. ~~It~~The *p50_gs* trait has been shown to play a key role in tree survival during severe droughts (Breshears et al., 2009; Rowland et al., 2015). The ability to withstand lower leaf water potentials is also a key indicator of sapling and seedling survival during drought and determines species distribution across a moisture gradient (Kursar et al., 2009). There may be a trade-off between drought tolerance (with a lower *p50_gs*) and drought avoidance (a less negative *p50_gs* but with a high capacitance; the amount of water released from reserves as leaf water potential declines), a crucial aspect in determining species drought resistance (Pineda-Garcia et al., 2013). Additionally, loss of conductivity was sensitive to the water potential at 50% loss of max conductivity within the stem (*p50_stem*) as it can largely affect the whole plant conductance and thus the water supply to the leaves. *p50_stem* negatively correlates with wood density and may be a marker of the trade-off between hydraulic efficiency and safety within the stem (Chen et al., 2009; Manzoni et al., 2013)~~. Even though we did not consider~~; however, other studies have shown that this trade-off ~~as we mainly focused on~~ is weak (Gleason et al., 2016). Liang et al (2019) showed that the ~~hydraulic traits in this study,~~strength of this trade-off could be ~~important to consider for competitions and co-existence among different plant functional types~~dependent on specie's drought strategies.

Leaf water potential and loss of conductance were both sensitive to the maximum xylem conductivity in the stem (*kmax_node_stem*). Higher maximum conductivity represents greater xylem efficiency, which in the absence of drought or light limitations would result in greater potential photosynthesis and less negative water potentials (Gleason et al., 2016). However, xylem with higher *kmax_node_stem* could be more vulnerable to embolism as water potential declines (Sperry and Love, 2015). In tropical rainforests, species with higher conductivity per unit leaf area generally are less desiccation~~-~~-tolerant, and thus exhibit higher mortality rates (Kursar et al., 2009). Low *kmax_node_stem* along with high leaf-to-sapwood area ratio (*la2sa*) also represents a vulnerability to reduced conductance which increases with height (Christoffersen et al., 2016).

Traits with lower order of impacts on water potential modulate the amount of stored water available during drought. ~~The fraction of water in the capillary reserve within the stem (f_{cap}) determines the amount of water stored within the stem. Water storage in the stem has been shown to help maintain higher water potentials as drought continues (Bartlett et al., 2019).~~ The bulk modulus of elasticity in the root (*epsil_node*~~)~~*_aroot*) together with root saturated water content determines the amount of water available from cellular storage between complete hydration and loss of turgor (Powell et al., 2017). This represents the ability of the roots to continually supply water to the rest of the plant as drought occurs. It also represents an investment in cellular structure, which may be an additional indicator of adaptations with non-hydraulic origin. The residual water content in the stem (*resid_node_stem*) determines the minimum amount of water xylem will hold and thus impact the amount of water storage plant can use during drought as well (Bartlett et al. 2012). In this study, we made the assumption that the traits are independent of each other, in order to understand the hydrodynamic behaviors of FATES-HYDRO for different hydraulic traits based on a single PFT. Understanding the trade-offs between these traits is crucial for determining the competition among different PFTs. Future studies would greatly benefit from assessing the significance of these trade-offs to predict vegetation dynamics under future climate change.

Formatted: Font color: Auto

-In contrast to the majority of hydraulic traits in the model, conduit taper, the fraction of total resistance belowground, and the leaf to sapwood area ratio are whole-plant hydraulic traits. Our analysis highlights the importance of whole-plant hydraulic traits such as conduit taper relative to tissue-level hydraulic traits for a range of plant hydraulic functions, including whole-plant conductance and hydraulic failure risks. An important area for future work is to better constrain and understand the consequences of intra- and interspecific variation in these whole-plant hydraulic traits in tropical forests. Our choice of the range of variation in the conduit taper exponent came from a study on temperate species, and was broad, encompassing the entire range of observed values in that study (Savage et al. 2010). Further, we estimated the effects of variation in the taper exponent on whole-plant conductance conditional on trees following a simple set of optimality assumptions (space-filling, area-conserving, and self-similar branching network structure). However, in practice, such assumptions are often not met (Smith et al., 2014). Therefore, it is possible that the model sensitivity to xylem taper in terms of whole-plant hydraulic function are overestimated. Nevertheless, our study highlights the importance of better constraining this parameter as well as further experimentation with alternate model structures to better account for non-optimal trees in tropical forests.

The sensitivity of vegetation to drought stress and hydraulic-failure-induced mortality is of paramount importance for understanding how ecosystems may respond to shifting temperature and rainfall patterns under a changing climate (Mcdowell et al., 2022). We recognize that parametric sensitivity could be different for different sites depending on climate driver, soil moisture and vegetation types. However, we expect the main parameter of importance ~~could be~~ could be useful to guide model calibration to select the candidate parameters for different sites. As understanding of plant hydrodynamics increases, linking model predictions to observable plant traits has emerged as a promising means of constraining predictions of ecosystem resilience. Such traits are challenging and costly to measure in the field and thus resources must be directed carefully when planning measurement campaigns. The identified parameters in this study could provide guidance on the limited measurement we could target in the field.

5. Acknowledgment

This research was supported as part of the Next Generation Ecosystem Experiments-Tropics, funded by the U.S. Department of Energy, Office of Science, Office of Biological and Environmental Research. RF acknowledges funding by the European Union's Horizon 2020 (H2020) research and innovation program under Grant Agreement No. 101003536 (ESM2025 – Earth System Models for the Future) and 821003 (4C, Climate-Carbon Interactions in the Coming Century).

6. CODE and Data Availability

The FATES-HYDRO code is available from https://doi.org/10.5281/zenodo.7686333. The traits data are in the supplementary file [traits_master_trop.csv].

7. Supplement Information

~~Two~~Three supplementary file are included. The HYDRO_DESCRIPTION.pdf provide the summary of the hydrodynamic implementation that is different from Christoffersen et al.

(2016). The traits_master_trop.csv file include all the hydraulic traits we assembled for the tropical region. The supplementary_figure.pdf provides additional figures for the main text.

8. Author contribution

CX and BC designed the sensitivity analysis experiments. BC collected the data and fitted the trait distributions. CX conducted the analysis and drafted the manuscript. BC, CX, RF, RN and CK designed the implementation of ~~HDRO~~HYDRO codes. -BC implemented the majority of ~~HDRO~~HYDRO codes with code improvement made by CX and RN.- ZR conducted the ensemble model simulations. MS provided the leaf cuticular conductance data. NM, CK and LK provided guidance on the sensitivity analysis, code development and trait data synthesis. All authors contributed to manuscript writing by providing edits and suggestions.

9. Competing interests

The contact author has declared that none of the authors has any competing interests.

Figures

Formatted: Font: Bold

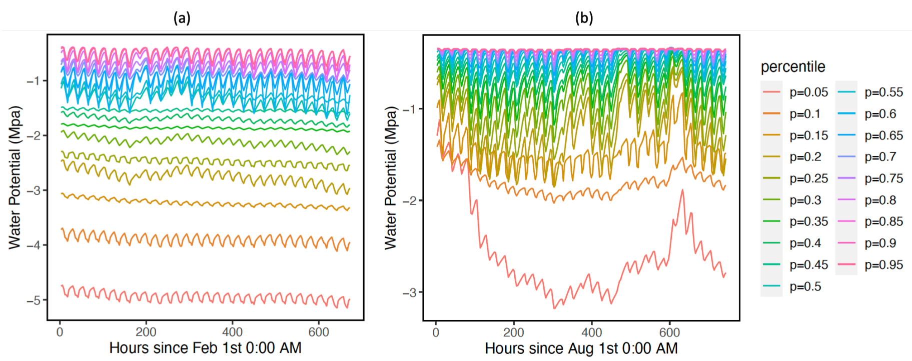

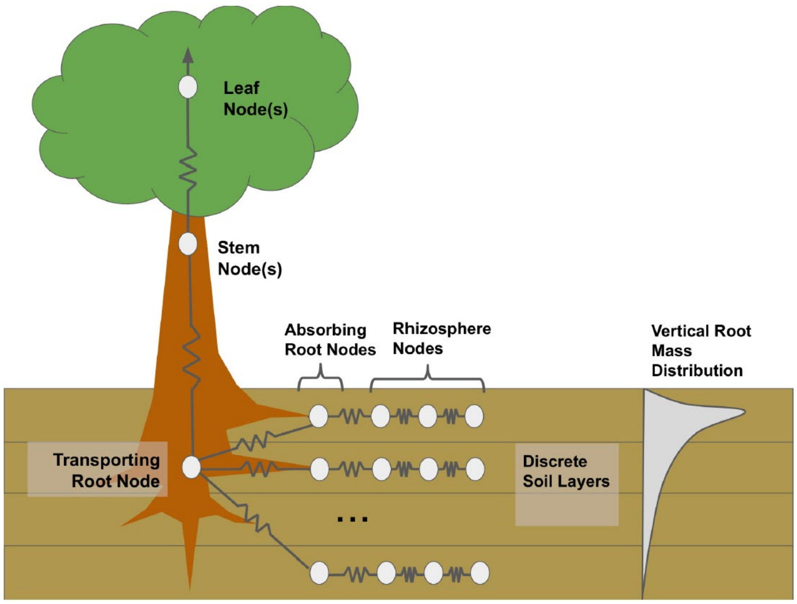

Figure 1: **Diagram of FATES-HYDO with simulation of rhizosphere shell, absorbing roots, transporting roots, stem and leaves.** The model is solved for different soil layers with different root distributions.

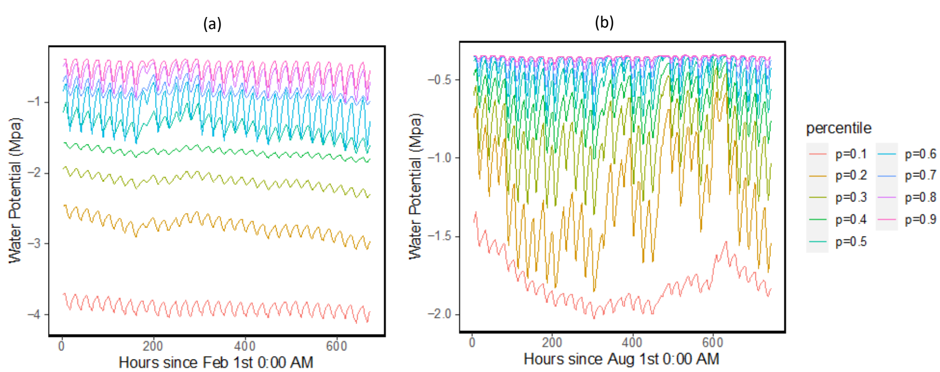

Figure 2: Simulated ranges of leaf water potential for February (a) and August (a), 2016 for trees with DBH > 60cm. The percentiles are calculated based on the monthly mean values of leaf water potentials for the 1000 ensemble simulations.

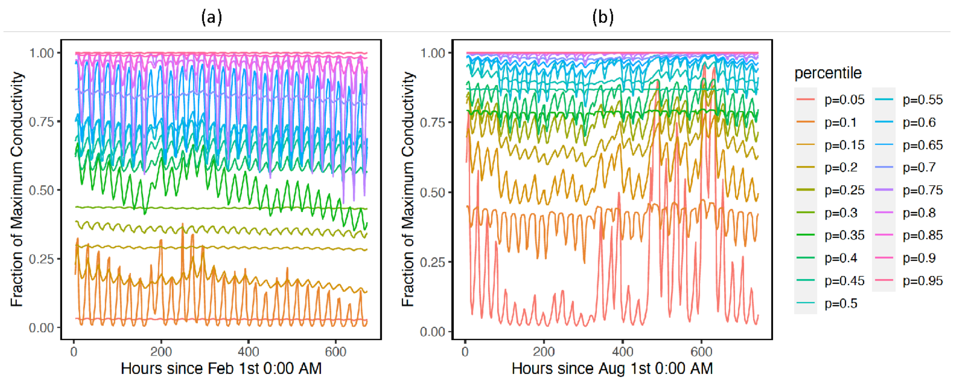

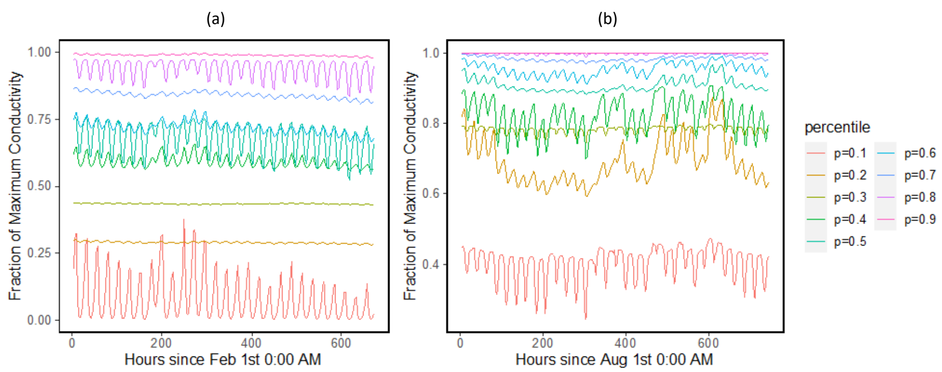

Figure ~~2~~3: Simulated ranges of fraction of maximum hydraulic conductivity of stem for February (a) and August (a), 2016~~.~~ for trees with DBH > 60cm. The percentiles are calculated based on the monthly mean values of leaf water potentials for the 1000 ensemble simulations.

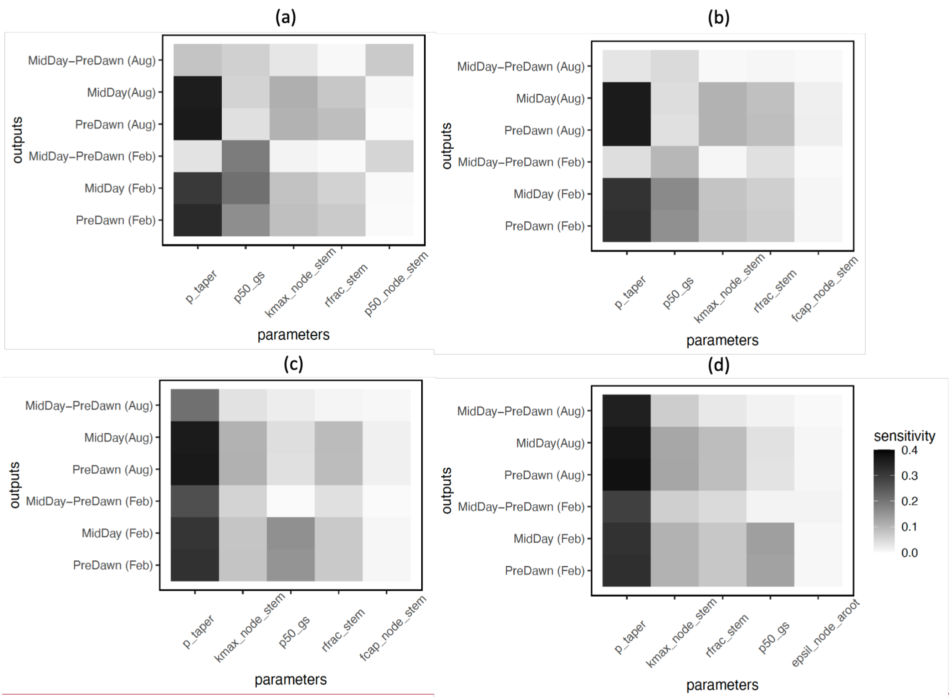
(a)
(b)
(c)
(d)
MidDay–PreDawn (Aug)
MidDay(Aug)
PreDawn (Aug)
MidDay–PreDawn (Feb)
MidDay (Feb)
PreDawn (Feb)
outputs
parameters
p_taper
p50_gs
kmax_node_stem
rfrac_stem
p50_node_stem
fcap_node_stem
epsil_node_aroot
sensitivity
0.4
0.3
0.2
0.1
0.0

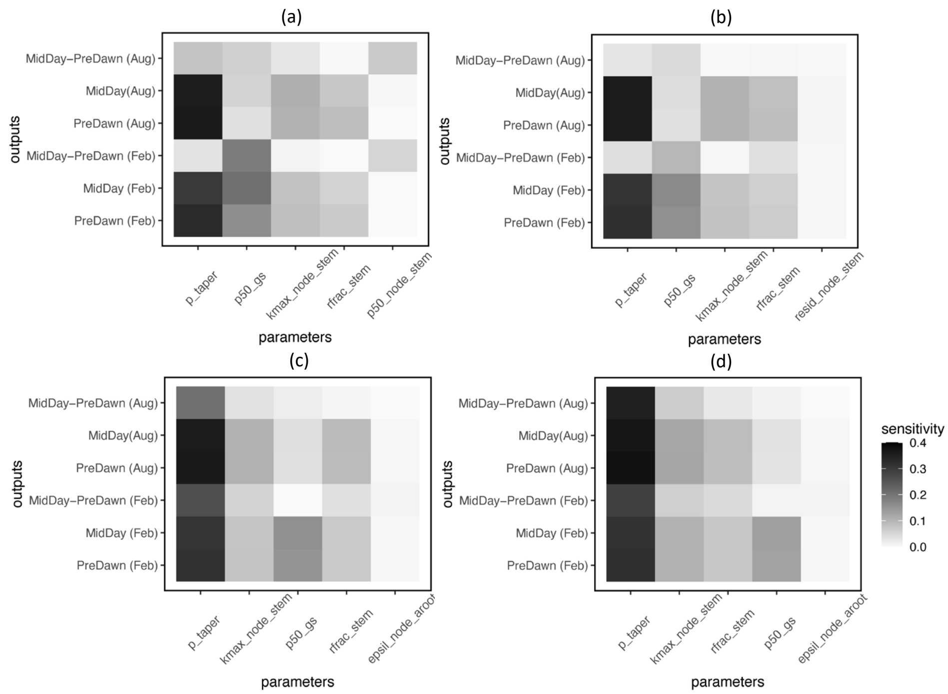

Figure 34: Key parameters that control simulated water potentials for leaf (a), stem (b), transporting root (c) and absorbing root (d).), for trees with DBH > 60cm. The sensitivity value refers to the proportion of total model output variance contributed by a specific parameter (0-1). See Table 1 for the explanation of the parameters.

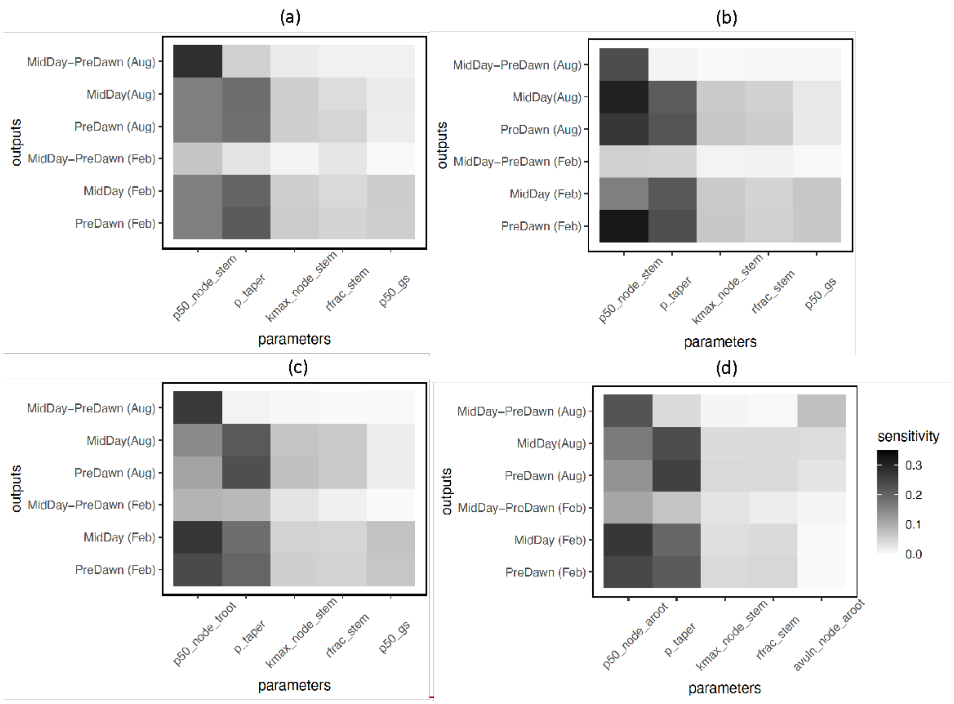
(a)
(b)
(c)
(d)
outputs
MidDay–PreDawn (Aug)
MidDay(Aug)
PreDawn (Aug)
MidDay–PreDawn (Feb)
MidDay (Feb)
PreDawn (Feb)
parameters
p50_node_stem
p_taper
kmax_node_stem
rfrac_stem
p50_gs
p50_node_troot
p50_node_aroot
avuln_node_aroot
sensitivity
0.3
0.2
0.1
0.0

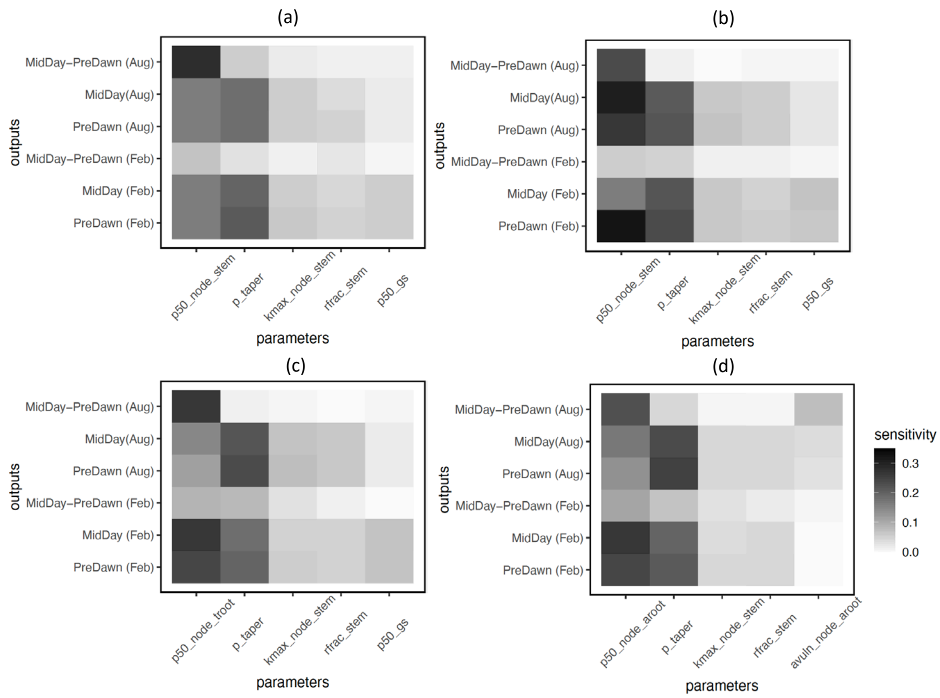

Figure 45: Key parameters that control simulated loss of conductivity for branch (a), stem (b), transporting root (c) and absorbing root (d).), for trees with DBH > 60cm. The sensitivity value refers to the proportion of total model output variance contributed by a specific parameter. See Table 1 for the explanation of the parameters. See Table 1 for the description of parameters.

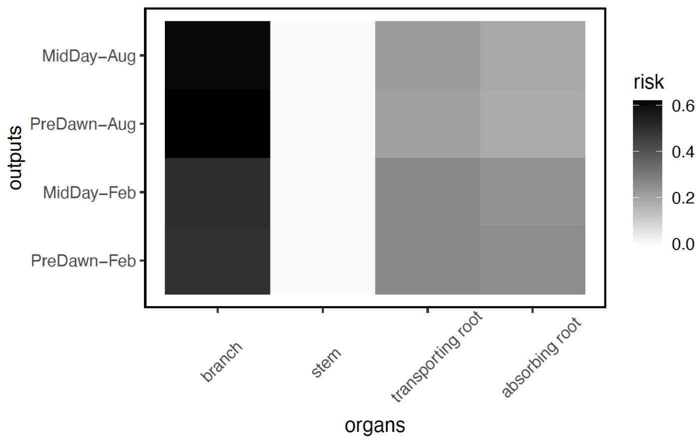

Figure ~~5~~6: Risk on the continuum for hydraulic failure as measured by percentage of total number of simulations with highest loss of conductivity for a specific organ (branch, stem, transporting root and absorbing root~~).~~), for trees with DBH > 60cm. As the model does not specifically simulate the branch, we calculated the risk of loss of conductivity based on the leaf water potential and hydraulic vulnerability curve from xylem.

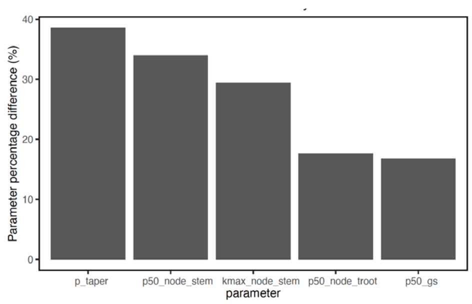

Figure ~~6~~7: Mean trait percentage difference for model ensemble simulations with loss of hydraulic conductivity larger than 50% and ensemble simulations with loss of hydraulic conductivity less than 50~~%.~~%, for trees with DBH > 60cm. See Table 1 for the description of parameters.

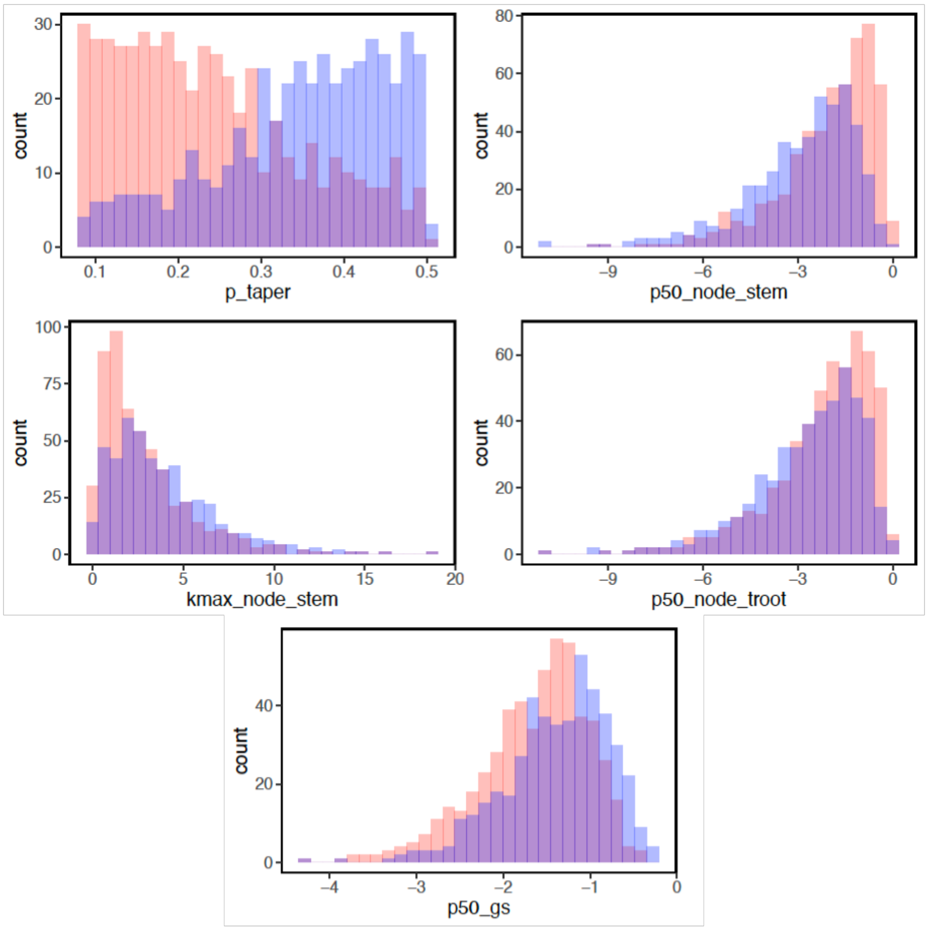

Figure ~~7~~8: Parameter difference for ensemble members with risk of mortality, for trees with DBH > 60cm. Blue bars indicate parameter values with lower mortality risk (<50% loss of hydraulic conductivity). Red bars indicate parameter values with higher mortality risk (>= 50% loss of hydraulic conductivity) and purple bars indicate parameter values stacked from transparent red/blue bars. See Table 1 for the description of parameters.

Table 1 Hydraulic parameters considered in the sensitivity analysis

PARAMETER (EQUATION NUMBER)	SYMBOL	UNITS	DISTRIBUTION[1]	SOURCES& NOTES
Pressure-Volume (PV) curve (water content – water potential relationship)				
saturated water content (thetas_node) (Eq. 5)	~~θ_s~~ $\theta_{sat,x}$	$cm^3\ cm^{-3}$	Leaf: Beta (9.69, 6.20) Stem: Beta (12.67, 7.4626) TRoot and AROOT: Beta (22.98, 5.29)	Christoffersen et al. (2016) Iversen et al. (2017) Wright et al. (2010) Roderick et al. (1999) Sack et al. (2003) Binks et al. (2016)
turgor loss point (tlp_node) (Eq. 5)	π_{tlp}	MPa	$\pi_{tlp} = (\pi_0\ \varepsilon)/(\pi_0 + \varepsilon)$	Bartlett et al. (2012~~);~~) ~~$\pi_{tlp} = (\pi_0\ \varepsilon)/(\pi_0 + \varepsilon)$~~
osmotic potential at full turgor (pinot_node) (Eq. 6)	π_0	MPa	Leaf: G [9.8,6.26], Stem, TRoot, ARoot: LN [0.32,0.39]	Bartlett et al. (2012, 2014, 2016) and Christoffersen et al. (2016)
bulk elastic modulus (epsil_node) (Eq. 7)	ε	MPa	Leaf: G (4.07, 4.12) Stem, TRoot and ARoot: G [3.57, 3.84]	Bartlett et al. (2012, 2014), and Christoffersen et al. (2016)
residual water fraction (resid_node) (Eq. 5)	RWC_r	unitless	Leaf: B [2.14,4.10] Stem, TRoot and ARoot: B [2.71, 4.53]	Bartlett et al. (2012, 2014), Christoffersen et al. (2016)
~~fraction of water in capillary reserve (fcap_node)~~	~~f_{cap}~~	~~unitless~~	~~U [0.1, 0.7]~~	~~Christoffersen et al. (2016)~~
VULNERABILITY CURVE (WATER POTENTIAL – HYDRAULIC CONDUCTIVITY RELATIONSHIP)				
water potential at 50% loss of max conductivity (p50_node) (Eq. 3)	$P_{50,x}$	MPa	Stem, TRoot and ARoot: G [2.07, 1.18]	Choat et al. (2012)
vulnerability curve shape parameter (avuln_node) (Eq. 3)	a_x	unitless	Stem, TRoot and ARoot: LN [0.82,0.66]	Choat et al. (2012)

Formatted Table

Formatted Table

xylem conductivity per unit sapwood area (kmax_node_stem) (Eq. 7)	$k_{s,max}$	kg m^{-1} s^{-1} MPa^{-1}	G [1.41, 2.37]	Choat et al. (2012)
Leaf hydraulics				
leaf water potential at 50% loss of max gs (p50_gs) (Eq. 11)	$P_{50,gs}$	MPa	G [5.73, 0.27]	Klein (2014)
stomatal vulnerability shape parameter(avuln_gs) (Eq. 11)	a_{gs}	unitless	a_{gs}= -2.406 P50,gs (-P50,gs) $^{-1.25}$	Christoffersen et al. (2016); derived according to empirical equation:)a_{gs}= -2.406 P50,gs (-P50,gs) $^{-1.25}$
Leaf cuticular conductivity (k0_leaf) (Eq. 10)	k0,r g_0	umol m^{-2}s^{-1}	LN [1.04, 0.84]	This study, based on (M. Slot, unpublished data measured by Martijn Slot)
Plant Hydraulic Architecture				
Xylem taper exponent for sapwood (p_taper) (Eq. 8)	p	(-)	U (0.08, 0.5)	Savage et al. (2010)
Leaf area to sapwood area ratio (la2sa) (Eq. 7)	la2sa $\frac{A_l}{A_s}$	(-)	LN (-0.48, 0.77)	Choat et al. (2012)
Root hydraulic Traits				
specific root length (*srl*) (Eq. 12)	srl	m g^{-1}	G [1.70, 35.31]	Iversen et al. (2017)
absorbing root radius (*rs2*) (Eq. 12)	r	mm	LN [-1.91, 0.79]	Iversen et al. (2017)
fraction of total tree resistance that is aboveground (*rfrac_stem*) (Eq. 9)	frac $R_{frac,stem}$	Unitless	U [0.1,0.7]	This study; empirical
root-soil interface conductivity per unit surface area (*Kr1*) (Eq. 13)	$k_{r1,max}$	kg m^{-1} s^{-1} MPa^{-1}	G [1.41, 2.37]	This study; empirically set the same as xylem conductivity
maximum root water loss rate (*Kr2*) (Eq. 13)	$k_{r2,max}$	kg m^{-1} s^{-1} MPa^{-1}	LN [-6.80, 0.92]	Wolfe (2020); Empirically set as 1/1000 bark water loss rate

Note: 1:B-Beta distribution; U- Uniform distribution [lower limit, upper limit]; N-Gaussian distribution (mean, standard deviation); LN-Log Normal Distribution [mean, standard deviation]; G-Gamma distribution (lambda, scale); TRoot-Transporting root; ARoot-Absorbing root.

Reference

~~1.~~ Adams, H. D., Zeppel, M. J. B., Anderegg, W. R. L., Hartmann, H., Landhausser, S. M., Tissue, D. T., Huxman, T. E., Hudson, P. J., Franz, T. E., Allen, C. D., Anderegg, L. D. L., Barron-Gafford, G. A., Beerling, D. J., Breshears, D. D., Brodribb, T. J., Bugmann, H., Cobb, R. C., Collins, A. D., Dickman, L. T., Duan, H. L., Ewers, B. E., Galiano, L., Galvez, D. A., Garcia-Forner, N., Gaylord, M. L., Germino, M. J., Gessler, A., Hacke, U. G., Hakamada, R., Hector, A., Jenkins, M. W., Kane, J. M., Kolb, T. E., Law, D. J., Lewis, J. D., Limousin, J. M., Love, D. M., Macalady, A. K., Martinez-Vilalta, J., Mencuccini, M., Mitchell, P. J., Muss, J. D., O'Brien, M. J., O'Grady, A. P., Pangle, R. E., Pinkard, E. A., Piper, F. I., Plaut, J. A., Pockman, W. T., Quirk, J., Reinhardt, K., Ripullone, F., Ryan, M. G., Sala, A., Sevanto, S., Sperry, J. S., Vargas, R., Vennetier, M., Way, D. A., Xu, C. G., Yepez, E. A., and McDowell, N. G.: A multi-species synthesis of physiological mechanisms in drought-induced tree mortality, Nat Ecol Evol, 1, 1285-1291, 10.1038/s41559-017-0248-x, 2017.

~~2.~~ Anderegg, W. R. L., Klein, T., Bartlett, M., Sack, L., Pellegrini, A. F. A., Choat, B., and Jansen, S.: Meta-analysis reveals that hydraulic traits explain cross-species patterns of drought-induced tree mortality across the globe, P Natl Acad Sci USA, 113, 5024-5029, 10.1073/pnas.1525678113, 2016.

~~3.~~ Anderegg, W. R. L., Konings, A. G., Trugman, A. T., Yu, K. L., Bowling, D. R., Gabbitas, R., Karp, D. S., Pacala, S., Sperry, J. S., Sulman, B. N., and Zenes, N.: Hydraulic diversity of forests regulates ecosystem resilience during drought, Nature, 561, 538–541, 10.1038/s41586-018-0539-7, 2018.

~~4.~~ Arora, V. K., Katavouta, A., Williams, R. G., Jones, C. D., Brovkin, V., Friedlingstein, P., Schwinger, J., Bopp, L., Boucher, O., Cadule, P., Chamberlain, M. A., Christian, J. R., Delire, C., Fisher, R. A., Hajima, T., Ilyina, T., Joetzjer, E., Kawamiya, M., Koven, C. D., Krasting, J. P., Law, R. M., Lawrence, D. M., Lenton, A., Lindsay, K., Pongratz, J., Raddatz, T., Seferian, R., Tachiiri, K., Tjiputra, J. F., Wiltshire, A., Wu, T. W., and Ziehn, T.: Carbon-concentration and carbon-climate feedbacks in CMIP6 models and their comparison to CMIP5 models, Biogeosciences, 17, 4173-4222, 10.5194/bg-17-4173-2020, 2020.

~~5.~~ Bartlett, M. K., ~~Detto, M., and Pacala, S. W.: Predicting shifts in the functional composition of tropical forests under increased drought and CO2 from trade-offs among plant hydraulic traits, Ecol Lett, 22, 67-77, 10.1111/ele.13168, 2019.~~

~~6.~~ ~~Bartlett, M. K.,~~ Scoffoni, C., and Sack, L.: The determinants of leaf turgor loss point and prediction of drought tolerance of species and biomes: a global meta-analysis, Ecol Lett, 15, 393-405, 10.1111/j.1461-0248.2012.01751.x, 2012.

~~7.~~ Bartlett, M. K., Klein, T., Jansen, S., Choat, B., and Sack, L.: The correlations and sequence of plant stomatal, hydraulic, and wilting responses to drought, P Natl Acad Sci USA, 113, 13098-13103, 10.1073/pnas.1604088113, 2016.

~~8.~~ Bartlett, M. K., Zhang, Y., Kreidler, N., Sun, S. W., Ardy, R., Cao, K. F., and Sack, L.: Global analysis of plasticity in turgor loss point, a key drought tolerance trait, Ecol Lett, 17, 1580-1590, 10.1111/ele.12374, 2014.

Bennett, A. C., McDowell, N. G., Allen, C. D., and Anderson-Teixeira, K. J.: Larger trees suffer most during drought in forests worldwide, Nat Plants, 1, Artn 15139 10.1038/Nplants.2015.139, 2015.

~~9.~~ Berenguer, E., Lennox, G. D., Ferreira, J., Malhi, Y., Aragao, L. E. O. C., Barreto, J. R., Espirito-Santo, F. D., Figueiredo, A. E. S., Franca, F., Gardner, T. A., Joly, C. A., Palmeira, A.

Formatted: No bullets or numbering

Formatted: No bullets or numbering

Formatted: No bullets or numbering

F., Quesada, C. A., Rossi, L. C., de Seixas, M. M. M., Smith, C. C., Withey, K., and Barlow, J.: Tracking the impacts of El Nino drought and fire in human-modified Amazonian forests, P Natl Acad Sci USA, 118, ARTN e2019377118: 10.1073/pnas.2019377118, 2021.

Bhagat, N., Raghav, M., Dubey, S., and Bedi, N.: Bacterial Exopolysaccharides: Insight into Their Role in Plant Abiotic Stress Tolerance, J Microbiol Biotechn, 31, 1045-1059, 10.4014/jmb.2105.05009, 2021.

~~10.~~ Binks, O., Meir, P., Rowland, L., da Costa, A. C. L., Vasconcelos, S. S., de Oliveira, A. A. R., Ferreira, L., Christoffersen, B., Nardini, A., and Mencuccini, M.: Plasticity in leaf-level water relations of tropical rainforest trees in response to experimental drought, New Phytol, 211, 477-488, 10.1111/nph.13927, 2016.

Formatted: No bullets or numbering

~~11.~~ Bonal, D., Burban, B., Stahl, C., Wagner, F., and Herault, B.: The response of tropical rainforests to drought-lessons from recent research and future prospects, Ann Forest Sci, 73, 27-44, 10.1007/s13595-015-0522-5, 2016.

~~12.~~ Bonan, G. B.: Forests and climate change: Forcings, feedbacks, and the climate benefits of forests, Science, 320, 1444-1449, 10.1126/science.1155121, 2008.

~~13.~~ Boyle, B., Hopkins, N., Lu, Z., Raygoza Garay, J. A., Mozzherin, D., Rees, T., Matasci, N., Narro, M. L., Piel, W. H., and Mckay, S. J.: The taxonomic name resolution service: an online tool for automated standardization of plant names, BMC bioinformatics, 14, 1-15, 2013.

~~14.~~ Breshears, D. D., Myers, O. B., Meyer, C. W., Barnes, F. J., Zou, C. B., Allen, C. D., McDowell, N. G., and Pockman, W. T.: Tree die-off in response to global change-type drought: mortality insights from a decade of plant water potential measurements, Front Ecol Environ, 7, 185-189, 10.1890/080016, 2009.

~~15.~~ Caldwell, P. M., Mametjanov, A., Tang, Q., Van Roekel, L. P., Golaz, J. C., Lin, W. Y., Bader, D. C., Keen, N. D., Feng, Y., Jacob, R., Maltrud, M. E., Roberts, A. F., Taylor, M. A., Veneziani, M., Wang, H. L., Wolfe, J. D., Balaguru, K., Cameron-Smith, P., Dong, L., Klein, S. A., Leung, L. R., Li, H. Y., Li, Q., Liu, X. H., Neale, R. B., Pinheiro, M., Qian, Y., Ullrich, P. A., Xie, S. C., Yang, Y., Zhang, Y. Y., Zhang, K., and Zhou, T.: The DOE E3SM Coupled Model Version 1: Description and Results at High Resolution, J Adv Model Earth Sy, 11, 4095-4146, 10.1029/2019ms001870, 2019.

~~16.~~ Chen, J. W., Zhang, Q., Li, X. S., and Cao, K. F.: Independence of stem and leaf hydraulic traits in six Euphorbiaceae tree species with contrasting leaf phenology, Planta, 230, 459-468, 10.1007/s00425-009-0959-6, 2009.

~~17.~~ Chitra-Tarak, R., Xu, C. G., Aguilar, S., Anderson-Teixeira, K. J., Chambers, J., Detto, M., Faybishenko, B., Fisher, R. A., Knox, R. G., Koven, C. D., Kueppers, L. M., Kunert, N., Kupers, S. J., McDowell, N. G., Newman, B. D., Paton, S. R., Perez, R., Ruiz, L., Sack, L., Warren, J. M., Wolfe, B. T., Wright, C., Wright, S. J., Zailaa, J., and McMahon, S. M.: Hydraulically-vulnerable trees survive on deep-water access during droughts in a tropical forest, New Phytol, 231, 1798-1813, 10.1111/nph.17464, 2021.

~~18.~~ Choat, B., Jansen, S., Brodribb, T. J., Cochard, H., Delzon, S., Bhaskar, R., Bucci, S. J., Feild, T. S., Gleason, S. M., Hacke, U. G., Jacobsen, A. L., Lens, F., Maherali, H., Martinez-Vilalta, J., Mayr, S., Mencuccini, M., Mitchell, P. J., Nardini, A., Pittermann, J., Pratt, R. B., Sperry, J. S., Westoby, M., Wright, I. J., and Zanne, A. E.: Global convergence in the vulnerability of forests to drought, Nature, 491, 752-+, 10.1038/nature11688, 2012.

~~19.~~ Christoffersen, B. O., Gloor, M., Fauset, S., Fyllas, N. M., Galbraith, D. R., Baker, T. R., Kruijt, B., Rowland, L., Fisher, R. A., Binks, O. J., Sevanto, S., Xu, C. G., Jansen, S., Choat, B., Mencuccini, M., McDowell, N. G., and Meir, P.: Linking hydraulic traits to tropical forest function in a size-structured and trait-driven model (TFS v.1-Hydro), Geosci Model Dev, 9, 4227-4255, 10.5194/gmd-9-4227-2016, 2016.

Dichio, B., Xiloyannis, C., Sofo, A., and Montanaro, G.: Osmotic regulation in leaves and roots of olive trees during a water deficit and rewatering, Tree Physiol, 26, 179-185, DOI 10.1093/treephys/26.2.179, 2006.

Fang, Y. L., Leung, L. R., Knox, R., Koven, C., and Bond-Lamberty, B.: Impact of the numerical solution approach of a plant hydrodynamic model (v0.1) on vegetation dynamics, Geosci Model Dev, 15, 6385-6398, 10.5194/gmd-15-6385-2022, 2022.

~~20.~~ Fisher, R., McDowell, N., Purves, D., Moorcroft, P., Sitch, S., Cox, P., Huntingford, C., Meir, P., and Woodward, F. I.: Assessing uncertainties in a second-generation dynamic vegetation model caused by ecological scale limitations, New Phytol, 187, 666-681, 10.1111/j.1469-8137.2010.03340.x, 2010.

~~21.~~ Fisher, R. A. and Koven, C. D.: Perspectives on the Future of Land Surface Models and the Challenges of Representing Complex Terrestrial Systems, J Adv Model Earth Sy, 12, ARTN e2018MS001453: 10.1029/2018MS001453, 2020.

~~22.~~ Fisher, R. A., Muszala, S., Verteinstein, M., Lawrence, P., Xu, C., McDowell, N. G., Knox, R. G., Koven, C., Holm, J., Rogers, B. M., Spessa, A., Lawrence, D., and Bonan, G.: Taking off the training wheels: the properties of a dynamic vegetation model without climate envelopes, CLM4.5(ED), Geosci Model Dev, 8, 3593-3619, 10.5194/gmd-8-3593-2015, 2015.

~~23.~~ Fisher, R. A., Koven, C. D., Anderegg, W. R. L., Christoffersen, B. O., Dietze, M. C., Farrior, C. E., Holm, J. A., Hurtt, G. C., Knox, R. G., Lawrence, P. J., Lichstein, J. W., Longo, M., Matheny, A. M., Medvigy, D., Muller-Landau, H. C., Powell, T. L., Serbin, S. P., Sato, H., Shuman, J. K., Smith, B., Trugman, A. T., Viskari, T., Verbeeck, H., Weng, E. S., Xu, C. G., Xu, X. T., Zhang, T., and Moorcroft, P. R.: Vegetation demographics in Earth System Models: A review of progress and priorities, Global Change Biol, 24, 35-54, 10.1111/gcb.13910, 2018.

~~24.~~ Gleason, S. M., Westoby, M., Jansen, S., Choat, B., Hacke, U. G., Pratt, R. B., Bhaskar, R., Brodribb, T. J., Bucci, S. J., Cao, K. F., Cochard, H., Delzon, S., Domec, J. C., Fan, Z. X., Feild, T. S., Jacobsen, A. L., Johnson, D. M., Lens, F., Maherali, H., Martinez-Vilalta, J., Mayr, S., McCulloh, K. A., Mencuccini, M., Mitchell, P. J., Morris, H., Nardini, A., Pittermann, J., Plavcova, L., Schreiber, S. G., Sperry, J. S., Wright, I. J., and Zanne, A. E.: Weak tradeoff between xylem safety and xylem-specific hydraulic efficiency across the world's woody plant species, New Phytol, 209, 123-136, 10.1111/nph.13646, 2016.

Hammond, W. M., Yu, K., Wilson, L. A., Will, R. E., Anderegg, W. R. L., and Adams, H. D.: Dead or dying? Quantifying the point of no return from hydraulic failure in drought-induced tree mortality, New Phytol, 223, 1834-1843, https://doi.org/10.1111/nph.15922, 2019.

~~25.~~ Hochberg, U., Rockwell, F. E., Holbrook, N. M., and Cochard, H.: Iso/Anisohydry: A Plant-Environment Interaction Rather Than a Simple Hydraulic Trait, Trends Plant Sci, 23, 112-120, 10.1016/j.tplants.2017.11.002, 2018.

~~26.~~ Huang, M. Y., Xu, Y., Longo, M., Keller, M., Knox, R. G., Koven, C. D., and Fisher, R. A.: Assessing impacts of selective logging on water, energy, and carbon budgets and ecosystem dynamics in Amazon forests using the Functionally Assembled Terrestrial Ecosystem Simulator, Biogeosciences, 17, 4999-5023, 10.5194/bg-17-4999-2020, 2020.

~~27.~~ Iversen, C. M., McCormack, M. L., Powell, A. S., Blackwood, C. B., Freschet, G. T., Kattge, J., Roumet, C., Stover, D. B., Soudzilovskaia, N. A., Valverde-Barrantes, O. J., van Bodegom, P. M., and Violle, C.: A global Fine-Root Ecology Database to address below-ground challenges in plant ecology, New Phytol, 215, 15-26, 10.1111/nph.14486, 2017.

Formatted: No bullets or numbering

Formatted: No bullets or numbering

~~28.~~ Kennedy, D., Swenson, S., Oleson, K. W., Lawrence, D. M., Fisher, R., da Costa, A. C. L., and Gentine, P.: Implementing Plant Hydraulics in the Community Land Model, Version 5, J Adv Model Earth Sy, 11, 485-513, 10.1029/2018ms001500, 2019.

~~29.~~ Klein, T.: The variability of stomatal sensitivity to leaf water potential across tree species indicates a continuum between isohydric and anisohydric behaviours, Funct Ecol, 28, 1313-1320, 10.1111/1365-2435.12289, 2014.

~~30.~~ Koven, C. D., Knox, R. G., Fisher, R. A., Chambers, J. Q., Christoffersen, B. O., Davies, S. J., Detto, M., Dietze, M. C., Faybishenko, B., Holm, J., Huang, M. Y., Kovenock, M., Kueppers, L. M., Lemieux, G., Massoud, E., McDowel, N. G., Muller-Landau, H. C., Needham, J. F., Norby, R. J., Powell, T., Rogers, A., Serbin, S. P., Shuman, J. K., Swann, A. L. S., Varadharajan, C., Walker, A. P., Wright, S. J., and Xu, C. G.: Benchmarking and parameter sensitivity of physiological and vegetation dynamics using the Functionally Assembled Terrestrial Ecosystem Simulator (FATES) at Barro Colorado Island, Panama, Biogeosciences, 17, 3017-3044, 10.5194/bg-17-3017-2020, 2020.

~~31.~~ Kunert, N., Zailaa, J., Herrmann, V., Muller-Landau, H. C., Wright, S. J., Perez, R., McMahon, S. M., Condit, R. C., Hubbell, S. P., Sack, L., Davies, S. J., and Anderson-Teixeira, K. J.: Leaf turgor loss point shapes local and regional distributions of evergreen but not deciduous tropical trees, New Phytol, 230, 485-496, 10.1111/nph.17187, 2021.

~~32.~~ Kursar, T. A., Engelbrecht, B. M. J., Burke, A., Tyree, M. T., El Omari, B., and Giraldo, J. P.: Tolerance to low leaf water status of tropical tree seedlings is related to drought performance and distribution, Funct Ecol, 23, 93-102, 10.1111/j.1365-2435.2008.01483.x, 2009.

Lambert, M. S. A., Tang, H., Aas, K. S., Stordal, F., Fisher, R. A., Fang, Y. L., Ding, J. Y., and Parmentier, F. J. W.: Inclusion of a cold hardening scheme to represent frost tolerance is essential to model realistic plant hydraulics in the Arctic-boreal zone in CLM5.0-FATES-Hydro, Geosci Model Dev, 15, 8809-8829, 10.5194/gmd-15-8809-2022, 2022.

Lawrence, D. M., Fisher, R. A., Koven, C. D., Oleson, K. W., Swenson, S. C., Bonan, G., Collier, N., Ghimire, B., van Kampenhout, L., Kennedy, D., Kluzek, E., Lawrence, P. J., Li, F., Li, H. Y., Lombardozzi, D., Riley, W. J., Sacks, W. J., Shi, M. J., Vertenstein, M., Wieder, W. R., Xu, C. G., Ali, A. A., Badger, A. M., Bisht, G., van den Broeke, M., Brunke, M. A., Burns, S. P., Buzan, J., Clark, M., Craig, A., Dahlin, K., Drewniak, B., Fisher, J. B., Flanner, M., Fox, A. M., Gentine, P., Hoffman, F., Keppel-Aleks, G., Knox, R., Kumar, S., Lenaerts, J., Leung, L. R., Lipscomb, W. H., Lu, Y. Q., Pandey, A., Pelletier, J. D., Perket, J., Randerson, J. T., Ricciuto, D. M., Sanderson, B. M., Slater, A., Subin, Z. M., Tang, J. Y., Thomas, R. Q., Martin, M. V., and Zeng, X. B.: The Community Land Model Version 5: Description of New Features, Benchmarking, and Impact of Forcing Uncertainty, J Adv Model Earth Sy, 11, 4245-4287, 10.1029/2018ms001583, 2019.

~~33.~~ Manzoni, S., Vico, G., Katul, G., Palmroth, S., Jackson, R. B., and Porporato, A.: Hydraulic limits on maximum plant transpiration and the emergence of the safety-efficiency trade-off, New Phytol, 198, 169-178, 10.1111/nph.12126, 2013.

~~34.~~ Massoud, E. C., Xu, C. G., Fisher, R. A., Knox, R. G., Walker, A. P., Serbin, S. P., Christoffersen, B. O., Holm, J. A., Kueppers, L. M., Ricciuto, D. M., Wei, L., Johnson, D. J., Chambers, J. Q., Koven, C. D., McDowell, N. G., and Vrugt, J. A.: Identification of key parameters controlling demographically structured vegetation dynamics in a land surface model: CLM4.5(FATES), Geosci Model Dev, 12, 4133-4164, 10.5194/gmd-12-4133-2019, 2019.

~~35.~~ McDowell, N., Allen, C. D., Anderson-Teixeira, K., Brando, P., Brienen, R., Chambers, J., Christoffersen, B., Davies, S., Doughty, C., Duque, A., Espirito-Santo, F., Fisher, R., Fontes,

Formatted: No bullets or numbering

C. G., Galbraith, D., Goodsman, D., Grossiord, C., Hartmann, H., Holm, J., Johnson, D. J., Kassim, A., Keller, M., Koven, C., Kueppers, L., Kumagai, T., Malhi, Y., McMahon, S. M., Mencuccini, M., Meir, P., Moorcroft, P., Muller-Landau, H. C., Phillips, O. L., Powell, T., Sierra, C. A., Sperry, J., Warren, J., Xu, C. G., and Xu, X. T.: Drivers and mechanisms of tree mortality in moist tropical forests, New Phytol, 219, 851-869, 10.1111/nph.15027, 2018.

McDowell, N. G., Fisher, R. A., Xu, C. G., Domec, J. C., Holtta, T., Mackay, D. S., Sperry, J. S., Boutz, A., Dickman, L., Gehres, N., Limousin, J. M., Macalady, A., Martinez-Vilalta, J., Mencuccini, M., Plaut, J. A., Ogee, J., Pangle, R. E., Rasse, D. P., Ryan, M. G., Sevanto, S., Waring, R. H., Williams, A. P., Yepez, E. A., and Pockman, W. T.: Evaluating theories of drought-induced vegetation mortality using a multimodel-experiment framework, New Phytol, 200, 304-321, 10.1111/nph.12465, 2013.

~~36.~~ McDowell, N. G., Sapes, G., Pivovaroff, A., Adams, H. D., Allen, C. D., Anderegg, W. R. L., Arend, M., Breshears, D. D., Brodribb, T., Choat, B., Cochard, H., De Caceres, M., De Kauwe, M. G., Grossiord, C., Hammond, W. M., Hartmann, H., Hoch, G., Kahmen, A., Klein, T., Mackay, D. S., Mantova, M., Martinez-Vilalta, J., Medlyn, B. E., Mencuccini, M., Nardini, A., Oliveira, R. S., Sala, A., Tissue, D. T., Torres-Ruiz, J. M., Trowbridge, A. M., Trugman, A. T., Wiley, E., and Xu, C. G.: Mechanisms of woody-plant mortality under rising drought, CO2 and vapour pressure deficit, Nat Rev Earth Env, 3, 294-308, 10.1038/s43017-022-00272-1, 2022.

~~37.~~ Moorcroft, P. R., Hurtt, G. C., and Pacala, S. W.: A method for scaling vegetation dynamics: The ecosystem demography model (ED), Ecol Monogr, 71, 557-585, 10.1890/0012-9615(2001)071[0557:Amfsvd]2.0.Co;2, 2001.

~~38.~~ Needham, J. F., Chambers, J., Fisher, R., Knox, R., and Koven, C. D.: Forest responses to simulated elevated CO2 under alternate hypotheses of size- and age-dependent mortality, Global Change Biol, 26, 5734-5753, 10.1111/gcb.15254, 2020.

Norman, J.: Modelling the complete crop canopy, in Modification of the Aerial Environment of Plants, Am. Soc. Agri. Eng. Monograph, 2, 249-277, 1979.

North, G. B. and Nobel, P. S.: Drought-Induced Changes in Hydraulic Conductivity and Structure in Roots of Ferocactus-Acanthodes and Opuntia-Ficus-Indica, New Phytol, 120, 9-19, DOI 10.1111/j.1469-8137.1992.tb01053.x, 1992.

Oleson, K. W., Lawrence, D. M., Bonan, G. B., Drewniak, B., Huang, M., Koven, C. D., Levis, S., Li, F., Riley, W. J., Subin, Z. M., Swenson, S. C., Thornton, P. E., Bozbiyik, A., Fisher, R., Heald, C. L., Kluzek, E., Lamarque, J.-F., Lawrence, P. J., Leung, L. R., Lipscomb, W., Muszala, S., Ricciuto, D. M., Sacks, W., Sun, Y., Tang, J., & Yang, Z.-L. : Technical description of version 4.5 of the Community Land Model (CLM) National Center for Atmospheric Research, Boulder, Colorado, USA.Tech. Rep. NCAR/TN-503+STR, 2013.

Olson, M. E., Anfodillo, T., Gleason, S. M., and McCulloh, K. A.: Tip-to-base xylem conduit widening as an adaptation: causes, consequences, and empirical priorities, New Phytol, 229, 1877-1893, 10.1111/nph.16961, 2021.

~~39.~~ Paton, S.: Yearly Reports_Barro Colorado Island, Smithsonian Tropical Research Institute, ~~https://doi.org/10.25573/data.11799111.v3~~https://doi.org/10.25573/data.11799111.v3, 2020.

~~40.~~ Pineda-Garcia, F., Paz, H., and Meinzer, F. C.: Drought resistance in early and late secondary successional species from a tropical dry forest: the interplay between xylem resistance to embolism, sapwood water storage and leaf shedding, Plant Cell Environ, 36, 405-418, 10.1111/j.1365-3040.2012.02582.x, 2013.

Formatted: No bullets or numbering

Formatted: No bullets or numbering

Poudel, M., Mendes, R., Costa, L. A., Bueno, C. G., Meng, Y., Folimonova, S. Y., Garrett, K. A., and Martins, S. J.: The role of plant-associated bacteria, fungi, and viruses in drought stress mitigation, Frontiers in microbiology, 12, 3058, 2021.

41. Powell, T. L., Wheeler, J. K., de Oliveira, A. A. R., da Costa, A. C. L., Saleska, S. R., Meir, P., and Moorcroft, P. R.: Differences in xylem and leaf hydraulic traits explain differences in drought tolerance among mature Amazon rainforest trees, Global Change Biol, 23, 4280-4293, 10.1111/gcb.13731, 2017.

42. Powell, T. L., Koven, C. D., Johnson, D. J., Faybishenko, B., Fisher, R. A., Knox, R. G., McDowell, N. G., Condit, R., Hubbell, S. P., Wright, S. J., Chambers, J. Q., and Kueppers, L. M.: Variation in hydroclimate sustains tropical forest biomass and promotes functional diversity, New Phytol, 219, 932-946, 10.1111/nph.15271, 2018.

43. Roderick, M. L., Berry, S. L., Saunders, A. R., and Noble, I. R.: On the relationship between the composition, morphology and function of leaves, Funct Ecol, 13, 696-710, DOI 10.1046/j.1365-2435.1999.00369.x, 1999.

Rodriguez-Zaccaro, F. D., Valdovinos-Ayala, J., Percolla, M. I., Venturas, M. D., Pratt, R. B., and Jacobsen, A. L.: Wood structure and function change with maturity: Age of the vascular cambium is associated with xylem changes in current-year growth, Plant, Cell & Environment, 42, 1816-1831, https://doi.org/10.1111/pce.13528, 2019.

44. Rowland, L., da Costa, A. C. L., Galbraith, D. R., Oliveira, R. S., Binks, O. J., Oliveira, A. A. R., Pullen, A. M., Doughty, C. E., Metcalfe, D. B., Vasconcelos, S. S., Ferreira, L. V., Malhi, Y., Grace, J., Mencuccini, M., and Meir, P.: Death from drought in tropical forests is triggered by hydraulics not carbon starvation, Nature, 528, 119-+, 10.1038/nature15539, 2015.

45. Sack, L., Cowan, P. D., Jaikumar, N., and Holbrook, N. M.: The 'hydrology' of leaves: co-ordination of structure and function in temperate woody species, Plant Cell Environ, 26, 1343-1356, DOI 10.1046/j.0016-8025.2003.01058.x, 2003.

46. Savage, V. M., Bentley, L. P., Enquist, B. J., Sperry, J. S., Smith, D. D., Reich, P. B., and von Allmen, E. I.: Hydraulic trade-offs and space filling enable better predictions of vascular structure and function in plants, P Natl Acad Sci USA, 107, 22722-22727, 10.1073/pnas.1012194108, 2010.

Schmidhalter, U.: The gradient between pre-dawn rhizoplane and bulk soil matric potentials, and its relation to the pre-dawn root and leaf water potentials of four species, Plant, Cell & Environment, 20, 953-960, https://doi.org/10.1046/j.1365-3040.1997.d01-136.x, 1997.

Seneviratne, S. I., Zhang, X., Adnan, M., Badi, W., Dereczynski, C., Luca, A. D., Ghosh, S., Iskandar, I., Kossin, J., Lewis, S., Otto, F., Pinto, I., Satoh, M., Vicente-Serrano, S. M., Wehner, M., Zhou, B., and Allan, R.: Weather and climate extreme events in a changing climate, in: Climate Change 2021: The Physical Science Basis: Working Group I contribution to the Sixth Assessment Report of the Intergovernmental Panel on Climate Change, edited by: Masson-Delmotte, V. P., Zhai, A., Pirani, S. L., and Connors, C., Cambridge University Press, Cambridge, UK, 1513-1766, 2021.

Shinozaki, K., Yoda, K., Hozumi, K., and Kira, T.: A quantitative analysis of plant form-the pipe model theory: I. Basic analyses, Japanese Journal of ecology, 14, 97-105, 1964.

Smith, D. D., Sperry, J. S., Enquist, B. J., Savage, V. M., McCulloh, K. A., and Bentley, L. P.: Deviation from symmetrically self-similar branching in trees predicts altered hydraulics, mechanics, light interception and metabolic scaling, New Phytol, 201, 217-229, 10.1111/nph.12487, 2014.

Formatted: No bullets or numbering

Formatted: No bullets or numbering

~~47.~~ Sperry, J. S. and Love, D. M.: What plant hydraulics can tell us about responses to climate-change droughts, New Phytol, 207, 14-27, 10.1111/nph.13354, 2015.

~~48.~~ Su, R., Liu, H., Wang, C., Zhang, H., and Cui, J.: Leaf turgor loss point is one of the best predictors of drought-induced tree mortality in tropical forest, Front Ecol Evol, 10, ARTN 974004: 10.3389/fevo.2022.974004, 2022.

Tyree, M. T. and Yang, S.: Water-storage capacity of Thuja, Tsuga and Acer stems measured by dehydration isotherms: the contribution of capillary water and cavitation, Planta, 182, 420-426, 1990.

Wei, L., Xu, C. G., Jansen, S., Zhou, H., Christoffersen, B. O., Pockman, W. T., Middleton, R. S., Marshall, J. D., and McDowell, N. G.: A heuristic classification of woody plants based on contrasting shade and drought strategies, Tree Physiol, 39, 767-781, 10.1093/treephys/tpy146, 2019.

~~49.~~ Wolfe, B. T.: Bark water vapour conductance is associated with drought performance in tropical trees, Biol Letters, 16, ARTN 20200263: 10.1098/rsbl.2020.0263, 2020.

~~50.~~ Wright, S. J., Kitajima, K., Kraft, N. J. B., Reich, P. B., Wright, I. J., Bunker, D. E., Condit, R., Dalling, J. W., Davies, S. J., Diaz, S., Engelbrecht, B. M. J., Harms, K. E., Hubbell, S. P., Marks, C. O., Ruiz-Jaen, M. C., Salvador, C. M., and Zanne, A. E.: Functional traits and the growth-mortality trade-off in tropical trees, Ecology, 91, 3664-3674, Doi 10.1890/09-2335.1, 2010.

~~51.~~ Xu, C. G. and Gertner, G.: Understanding and comparisons of different sampling approaches for the Fourier Amplitudes Sensitivity Test (FAST), Comput Stat Data An, 55, 184-198, 10.1016/j.csda.2010.06.028, 2011a.

~~52.~~ Xu, C. G. and Gertner, G. Z.: Reliability of global sensitivity indices, J Stat Comput Sim, 81, 1939-1969, 10.1080/00949655.2010.509317, 2011b.

~~53.~~ Xu, C. G., McDowell, N. G., Fisher, R. A., Wei, L., Sevanto, S., Christoffersen, B. O., Weng, E. S., and Middleton, R. S.: Increasing impacts of extreme droughts on vegetation productivity under climate change, Nat Clim Change, 9, 948-+, 10.1038/s41558-019-0630-6, 2019.

~~54.~~ Xu, X. T., Medvigy, D., Powers, J. S., Becknell, J. M., and Guan, K. Y.: Diversity in plant hydraulic traits explains seasonal and inter-annual variations of vegetation dynamics in seasonally dry tropical forests, New Phytol, 212, 80-95, 10.1111/nph.14009, 2016.

~~55.~~ Yang, S. D. and Tyree, M. T.: Hydraulic Resistance in Acer-Saccharum Shoots and Its Influence on Leaf Water Potential and Transpiration, Tree Physiol, 12, 231-242, DOI 10.1093/treephys/12.3.231, 1993.

Formatted: No bullets or numbering

Formatted: No bullets or numbering